

Stony Brook University



OFFICIAL COPY

The official electronic file of this thesis or dissertation is maintained by the University Libraries on behalf of The Graduate School at Stony Brook University.

© All Rights Reserved by Author.

Robust Self-Optimization of Handover in Wireless Systems

A Dissertation Presented

by

Gun-Yeob Kim

to

The Graduate School

in Partial Fulfillment of the

Requirements

for the Degree of

Doctor of Philosophy

in

Electrical Engineering

Stony Brook University

May 2010

Stony Brook University

The Graduate School

Gun-Yeob Kim

We, the dissertation committee for the above candidate for the
Doctor of Philosophy degree,
hereby recommend acceptance of this dissertation.

Sangjin Hong, Dissertation Advisor
Professor, Department of Electrical & Computer Engineering

Dmitri Donetski, Chairperson of Defense
Professor, Department of Electrical & Computer Engineering

Milutin Stanacevic,
Professor, Department of Electrical and Computer Engineering

Hongshik Ahn,
Professor, Department of Applied Mathematics and Statistics

This dissertation is accepted by the Graduate School

Lawrence Martin
Dean of the Graduate School

Abstract of the Dissertation

Robust Self-Optimization of Handover in Wireless Systems

by

Gun-Yeob Kim

Doctor of Philosophy

in

Electrical Engineering

Stony Brook University

2010

This thesis presents a cellular radio network design and operating guideline based on LTE-Advanced (LTE-A) technology to improve the cell edge user performance. Coordinated Multi-Point (CoMP) transmission / reception is being studied in LTE-A to provide seamless mobility. This study derived macro-diversity gain based on a mathematical analysis for multiple deployment scenarios including homogeneous and heterogeneous networks. And we characterized RF propagation parameters to support a seamless handover based on collaborative transmission.

Support of soft handover is essential for improving the performance of cell edge users. This study evaluates the soft handover gain in LTE-A downlink. Reference signal received power (RSRP) is used to define the triggers and the measurements

for soft handover. Pathloss, intra-cell and inter-cell interference are modeled and are characterized for the calculation of handover gain. Mathematical analysis in terms of SINR gain and HO margin between soft handover and hard handover is performed in a CoMP set. The results show that propagation parameters significantly affect the choice of the handover margin and the SINR performance.

Heterogeneous network deployment scenarios are also being studied in the LTE-A. One of objectives is to provide seamless mobility in the mixed case of macro and pico eNBs in co-channel deployment scenario where the RF coverage areas may be overlapped. Support of heterogeneous network will require the modification of radio link connection approach due to coverage imbalance between DL and UL by the different transmit powers of macro and pico eNBs. In a conventional network including LTE, the UE is typically connected to the cell that provides the strongest DL signal power. However, the UE suffers from strong interference due to UL/DL link imbalance in a heterogeneous network. We investigate possible solutions to address this issue based on analytical framework and characterized RF parameters based on collaborative transmission.

To Jenny, James, and Chris

Contents

List of Figures	ix
1 Introduction	1
2 Background	4
2.1 Coordinated Multi-point Transmission	4
2.1.1 Downlink CoMP Schemes	5
2.1.2 CoMP Feedback Signals	6
2.2 Heterogeneous Network	7
2.2.1 Generic Scenarios of Heterogeneous Network Deployment	7
2.2.2 Characteristics of Heterogeneous Network	9
2.2.3 Resource Allocation and Coordination	10
2.2.4 Measurement for Cell Selections and Handover	11
3 Analysis of Macro-Diversity in LTE-Advanced	13
3.1 Introduction	13
3.2 CoMP Models and Assumptions	15
3.2.1 CoMP Set	15
3.2.2 System Scenario	16
3.3 Downlink Interference Analysis	18
3.3.1 Intra-cell Interference	19

3.3.2	Inter-cell Interference	21
3.4	Analysis of Hard and Soft Handovers	22
3.4.1	Hard Handover Analysis	22
3.4.2	Soft Handover Analysis	23
3.5	Numerical Results	25
3.6	Conclusion	27
4	Optimized Handover for Heterogeneous Network Deployment in LTE-Advanced	34
4.1	Introduction	34
4.2	Heterogeneous Network Models and Assumptions	36
4.2.1	CoMP Set in Heterogeneous Network	37
4.2.2	Propagation Parameters	38
4.2.3	Power Parameters	41
4.3	Downlink Interference Analysis in Heterogeneous Network	43
4.3.1	Intra-cell Interference in Heterogeneous Network	44
4.3.2	Inter-cell Interference in Heterogeneous Network	46
4.4	Analysis of Hard and Soft Handover in Heterogeneous Network	48
4.4.1	Hard Handover Analysis	49
4.4.2	Soft Handover Analysis	51
4.5	Numerical Results	54
4.6	Conclusion	57
5	Conclusion and Future Research	69
5.1	Conclusion	69

5.2 Future research 70

Bibliography 71

List of Figures

2-1	Heterogeneous Network and RF coverage.	8
3-1	CoMP Set.	16
3-2	System Model.	18
3-3	Assumption for Interference Analysis (a) Resource allocation by Semi-Static Scheduler (b) Example of User allocation in eNBs and (c) Multi-point reception with interference.	28
3-4	SINR depending on distance $r_{i,0}/D_{i,1}$ ($m=3$, $\sigma=8$, and $\varepsilon=0.05$)	29
3-5	SINR depending on distance $r_{i,0}/D_{i,1}$ ($m=4$, $\sigma=8$, and $\varepsilon=0.05$)	30
3-6	SINR versus M_{SH} for different values of ε	31
3-7	SINR versus M_{SH} for different values of pathloss exponent m	32
3-8	SINR versus M_{SH} for different values of σ	33
4-1	Heterogeneous CoMP Set.	38
4-2	System Model.	40
4-3	Macro eNB RSRP and Pathloss Curve.	43
4-4	Pico eNB RSRP and Pathloss Curve.	44
4-5	Pico and eNB placement and scenario.	45

4-6	SINR depending on distance $r_{i,0}$ ($d=200\text{meter}$, $\text{Power}=[46,46,37]$, $\sigma=8$, and $\varepsilon=0.05$)	58
4-7	SINR depending on distance $r_{i,0}$ ($d=300\text{meter}$, $\text{Power}=[46,46,37]$, $\sigma=8$, and $\varepsilon=0.05$)	59
4-8	SINR depending on distance $r_{i,0}$ ($d=400\text{meter}$, $\text{Power}=[46,46,37]$, $\sigma=8$, and $\varepsilon=0.05$)	60
4-9	SINR depending on distance $r_{i,0}$ ($d=200\text{meter}$, $\text{Power}=[46,46,34]$, $\sigma=8$, and $\varepsilon=0.05$)	61
4-10	SINR depending on distance $r_{i,0}$ ($d=200\text{meter}$, $\text{Power}=[46,46,25]$, $\sigma=8$, and $\varepsilon=0.05$)	62
4-11	SINR depending on distance $r_{i,0}$ ($d=300\text{meter}$, $\text{Power}=[46,46,34]$, $\sigma=8$, and $\varepsilon=0.05$)	63
4-12	SINR depending on distance $r_{i,0}$ ($d=300\text{meter}$, $\text{Power}=[46,46,28]$, $\sigma=8$, and $\varepsilon=0.05$)	64
4-13	SINR versus M_{SH} for different values of Power at 200meter ($d=300\text{meter}$, $\sigma=8$, and $\varepsilon=0.05$)	65
4-14	SINR versus M_{SH} for different values of ε at 120meter ($d=300\text{meter}$, $\sigma=8$, and $\text{Power}=[46,34,34]$)	66
4-15	SINR versus M_{SH} for different values of ε at 500meter ($d=300\text{meter}$, $\sigma=8$, and $\text{Power}=[46,34,34]$)	67
4-16	SINR versus M_{SH} for different values of ρ at 120meter ($d=300\text{meter}$, $\sigma=8$, and $\text{Power}=[46,34,34]$)	68

Chapter 1

Introduction

3GPP Long-Term Evolution (LTE) is based on Orthogonal Frequency Division Multiple Access (OFDMA) technology and hard handover is supported for the LTE systems using L3-filter, hysteresis, and time-to-trigger mechanisms. One of the main goals of UTRAN LTE is to provide seamless access to voice and multimedia services with strict latency requirements which is achieved by the current technology, however inter NodeB macro-diversity is not supported. Currently Coordinated Multi-Point (CoMP) transmission / reception is being studied in LTE-A for further evolution of 3GPP LTE and it is foreseen that LTE-A will use soft handover to improve the performance of cell edge users. Hence, the study of handover and its associated RF characteristics is required to select and control the system resources much more effectively in LTE-A technology.

The next generation networking will bring an increasing heterogeneity of technologies and an increasing networking complexity and dynamics. Recently the Self Organizing Network (SON) is introduced as part of the LTE and it is a promising

approach to maximize total performance of networks. This enables spontaneous, autonomous networks among mobile devices, and it also helps conventional network operators reduce the administrative need and complexity in network installation, maintenance, and management. One of areas in Self-Optimization is about Mobility robustness optimization. To eliminate unnecessary handover and to provide appropriate handover timing, this optimization automatically adjusts the thresholds related to cell reselection and handover [1], [2], [3].

In this dissertation, we characterized handover margin and its associated RF characteristics in LTE-A since this analytic data can be exploited to handover parameter selection and network optimization in SON.

Mobile wireless systems including LTE systems are vulnerable to the shadow fading phenomenon which has a log-normal distribution. To provide adequate coverage to the area being served by a eNB the transmit power needs to be raised by some amount over the level required to overcome the distance loss. The amount by which the transmit power needs to be raised to account for shadow fading is known as the fade margin. The LTE system which allow soft handover are believed to require smaller fade margins than other systems in which mobiles have to experience hard handover to switch over to better quality legs [4].

The other key components which should be considered are power, propagation and loading parameters. soft handover ratio is one of the most parameters for the performance analysis of cellular system. A low soft handover ratio reduces the macro-diversity gain while a high soft handover ratio increases the macro-diversity gain to some extent at the expense of network resource consumption, which will both reduce

the capacity and degrade the network performance. At this time, it is necessary to adjust the soft handover parameters in accordance with the actual network traffic loads to keep the soft handover ratio within the proper range. Therefore we first need to derive an analytical expression of the soft handover gain in the propagation environment with shadow fading [5].

The remainder of this dissertation is organized as follows: Chapter 2 reviews the CoMP technology and Heterogeneous network. In Chapter 3, we derived the soft handover gain in LTE-A homogeneous network. Pathloss, intra-cell and inter-cell interference are modeled and are taken into account for the calculation of handover gain in CoMP set. In Chapter 4, we studied Heterogeneous network deployment scenarios in the mixed case of macro and pico eNBs in co-channel deployment scenario where the RF coverage areas may be overlapped. We investigate possible solutions to address this issue based on analytical framework and characterized RF parameters based on collaborative transmission. Chapter 5 finally concludes the research works in this dissertation, and mention the future works.

Chapter 2

Background

2.1 Coordinated Multi-point Transmission

3GPP LTE is designed to be deployed in frequency reuse-1. This allows operators to deploy the network without extensive frequency planning. However reuse-1 can suffer from high inter-cell interference, adversely affecting cell coverage area and cell edge user data rate. In LTE Release 8, intercell interference coordination (ICIC) schemes such as fractional frequency reuse (FFR) or soft fractional frequency reuse (SFFR) are feasible by incorporating limited X2 interface between the base stations: Overload Indicator (OI) and High Interference Indicator (HII) are exchanged to support ICIC for uplink and Relative Narrowband Transmit Power (RNTP) exchange allows downlink interference coordination. These schemes create favorable interference condition in a portion of the frequency, allowing increased coverage and cell edge data rate [12].

Coordinated Multi-Point (CoMP) transmission / reception being studied in LTE-A extends this capability by allowing nodes in multiple sites to participate in transmis-

sion/reception of user data. Information theory on Network MIMO promises great potential for enhanced edge user data rate, coverage and cell throughput. Performance of CoMP scheme highly depends on the backhaul availability. It is foreseen that evolution of backhaul technology can accommodate increased backhaul requirements of CoMP in LTE-A deployment timeframe. It is noted that different backhaul technologies will coexist, requiring different CoMP schemes optimized for available backhaul. CoMP schemes are categorized depending on backhaul latency and channel state information (CSI) / data availability in neighboring cells.

2.1.1 Downlink CoMP Schemes

Coordinated multi-point transmission and reception (CoMP) is one of the key techniques for LTE-Advanced. The following CoMP categories have been agreed in the recent Standard.

For Joint Processing (JP), data is available at each point in CoMP cooperating set. Cooperating set is the set of points directly or indirectly participating in PDSCH transmission to UE. Note that this set may or need not be transparent to the UE. Joint Processing has 2 categories. The first one is Joint Transmission - PDSCH transmission from multiple points (part of or entire CoMP cooperating set) at a time. Data to a single UE is simultaneously transmitted from multiple transmission points, e.g. to (coherently or non-coherently) improve the received signal quality and/or cancel actively interference for other UEs. The second one is Dynamic cell selection - PDSCH transmission from one point at a time (within CoMP cooperating set)

For Coordinated Scheduling/Beamforming (CS/CB), data is only available at serving cell (data transmission from that point) but user scheduling/beamforming decisions are made with coordination among cells corresponding to the CoMP cooperating set [18].

2.1.2 CoMP Feedback Signals

The three main categories of CoMP feedback mechanisms have been identified to be: 1) Explicit channel state/statistical information feedback. (Channel as observed by the receiver, without assuming any transmission or receiver processing) 2) Implicit channel state/statistical information feedback (feedback mechanisms that use hypotheses of different transmission and/or reception processing, e.g., CQI/PMI/RI) 3) UE transmission of SRS can be used for CSI estimation at eNB exploiting channel reciprocity [24].

Combinations of full or subset of above three are possible. Look at these types of feedback mechanisms for the evaluations. UL overhead (number of bits) associated with each specific feedback mechanism needs to be identified. The feedback overhead (UL) vs, DL performance tradeoff should be assessed with the goal to target minimum overhead for a given performance. For the CoMP schemes that require feedback, individual per-cell feedback is considered as baseline. Complementary inter-cell feedback might be needed. UE CoMP feedback reports target the serving cell (on UL resources from serving cell) as baseline when X2 interface is available and is adequate for CoMP operation in terms of latency and capacity. In this case, the reception of

UE reports at cells other than the serving cell is a network implementation choice. The feedback reporting for cases with X2 interface not available or not adequate (latency and capacity), and for cases where feedback reports to the serving cell causes large interference (e.g., in heterogeneous deployment scenarios) for CoMP operation needs to be discussed and, if found needed, a solution needs to be identified.

2.2 Heterogeneous Network

The system design and performance evaluation of 3GPP LTE radio access networks (RAN) have so far been generally based on homogeneous cell layouts. Heterogeneous network configurations have now been included in the LTE-A study item [6]. The objective in [6] is to improve the overall capacity by deploying additional network nodes within the local-area range, such as low-power micro/pico eNBs, home eNB/CSG cells and relay nodes.

2.2.1 Generic Scenarios of Heterogeneous Network Deployment

A heterogeneous network in the context of LTE is a network containing network nodes, such as eNBs, with different characteristics such as transmission power and RF coverage area. eNBs with different transmission powers are used to support large and small RF coverage areas. The macro eNB with a large RF coverage area is deployed in a planned way for blanket coverage of urban, suburban, or rural areas. The local nodes with small RF coverage areas aim to complement the macro eNB for

coverage extension or throughput enhancement.

The RF coverage areas of the heterogeneous network nodes could be overlapped or disjoint as shown in Fig. 2-1. The overlapped RF coverage design of large cells and small cells, which is shown in blue and yellow in Fig. 2-1, aims to enhance the system performance in throughput, accessibility, privacy and service. The design of disjoint RF coverage areas in heterogeneous networks, as shown in red in Fig. 2-1, intends to extend the RF coverage area to smaller local regions and fill coverage holes.

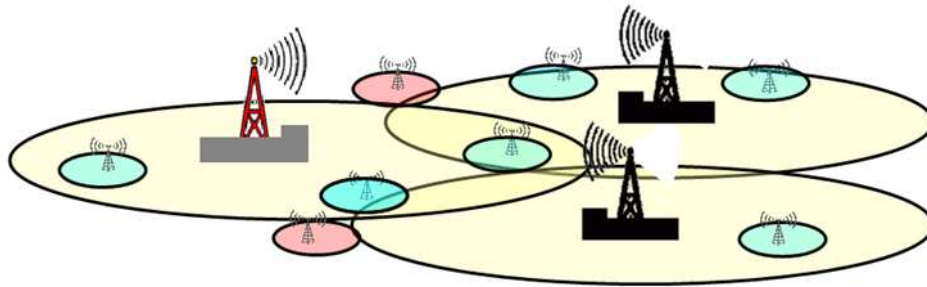


Figure 2-1: Heterogeneous Network and RF coverage.

The deployment scenarios of heterogeneous networks include coverage extension to minimize coverage holes, wireless extension to small regions or moving regions, small area cell splitting for non-homogeneous user distribution, hot spot coverage, extension of indoor coverage, and small private wireless networks for home users or enterprises. Heterogeneous network applications include non-homogeneous cell deployment by operators and hybrid network deployment of public and private/semi-private networks.

The LTE-A system design to support heterogeneous network deployment depends on the characteristics of the required network nodes, including operation, functional distribution and network management.

2.2.2 Characteristics of Heterogeneous Network

The heterogeneous network deployment is characterized by the types and location of local eNBs embedded in the macro eNB coverage areas. Different types of local eNBs are deployed along with macro eNBs based on the needs of different applications, services, and coverage areas.

The deployment of both macro cells and micro/pico cells is intended to cover areas with non-homogeneous user distributions in a geographical area, such as hot spots, highway toll booths, sports stadia, airports, train stations, and indoor arenas. The micro/pico cells are used to cover the areas of high density of mobile users to compensate for the insufficiency of the radio resources from the macro eNBs. The deployment of micro/pico cells along with macro cells could be done through non-homogeneous cell splitting, with the macro eNBs and micro/pico eNBs having their own coverage area. Since the co-deployments of macro and micro/pico cells are planned by operators, the network configuration in the UE could be configured appropriately to allow access. The operators could also perform system planning and RF optimization for the micro/pico cell splitting with macro cells

The micro/pico cells could also overlay with the macro cells to have an overlapped coverage area. When the coverage area of macro and micro/pico cells are overlapped, the algorithms, procedures and parameters based on RF signal strength/quality need to be re-designed since both macro cells and micro/pico cells experience strong intra-cell co-channel interference. The initial access and handover procedures need to be enhanced to optimize the performance in access availability, access delay, service

continuity and network load balance. Further studies are also required in resource allocation and interference management to mitigate the intra-cell co-channel interference.

2.2.3 Resource Allocation and Coordination

The target of the resource allocation and coordination in the heterogeneous network is to maximize the distance between co-channels in order to minimize the co-channel interference. Since the heterogeneous network is characterized by the coexistence or overlay of macro eNB and local eNB, the radio resource allocation between the macro eNB and micro/pico, relay or home eNB needs to be coordinated to mitigate the co-channel interference. This is extremely important when micro/pico eNB, relay nodes, and home eNBs overlay with macro eNB.

The coordination of the radio resource in the heterogeneous network could be realized by allocating different resources between neighboring eNBs in different time, frequency or power to mitigate the co-channel interference. The strategy of coordinating radio resource allocation strongly depends on the controllability of the macro eNBs to the local eNBs. In the scenario of micro/pico eNBs overlaying with macro eNB, the radio resource could be allocated jointly or in coordination to minimize the co-channel interference. For the home eNB and mobile relay deployment, it is a challenge for resource coordination since the location and coverage areas of home eNB and mobile relay are uncertain. Thus, distributed resource allocation with randomization or static/semi-static coordination is desired to minimize the co-channel interference.

The resource allocation strategies could be categorized into autonomous and planned carrier selection in multiple carrier aggregation cases with detailed discussion in the following

Autonomous resource allocation and carrier aggregation - The autonomous carrier selection is for the home eNB to select the carriers autonomously. The autonomous carrier selection could be done arbitrarily by the home eNB or in a sophisticated manner through a selection algorithm by the home eNB.

Planned resource allocation and carrier aggregation - The planned resource allocation for multiple carriers includes static carrier selection and random carrier selection for home eNBs. Static carrier selection is planned and assigned by the operator, which is similar to fractional frequency reuse. The random carrier selection involves the home eNB selecting the carriers in a random pattern from available carriers provided by the operator. The random pattern could be provided by the operator to minimize possible co-channel interference or generated (pseudo-)randomly from the home eNB itself.

2.2.4 Measurement for Cell Selections and Handover

Cell selection in heterogeneous networks is quite different to that of homogeneous networks. The cell selection criterion is based on the UE received signal power or quality. The received signal power or quality would work when the coverage area is slightly overlapped or disjoint. It would not work properly when the local cell and macro cell are overlaid. Since the local cells are overlaid on the macro cell, the UE

will measure PSS/SSS and CRS with high interference from the overlaid cells. The measurement events based on CRS power/quality and procedures for cell selection and handover in Rel-8 would need to be enhanced in the heterogeneous network. The possible enhancements in measurement events and procedures to support cell selection and handover for heterogeneous network are:

Assistance information related to the interference source for measurement events - The serving cell provides the CRS information for the interfered cells in the overlaid deployment scenario. The UE would estimate the interference and take it into account in the measurement event for cell selection and handover.

Measurements for heterogeneous networks - The current UE measurements RSRP and RSRQ are wideband measurements. In order to support some interference management schemes for data traffic and improving hearability of DL control channel, new measurements, such as narrow band measurement for FFR, might be needed. The detail of such measurements should be discussed in the work item phase.

Procedures for heterogeneous networks - In order to support measurement and interference management, such as coordinated muting or softening, the DL transmitted power of the data, control channel, and RS, at the macro cell or local cells might be power controlled. The procedure of transmission power control could be defined for autonomous interference management for heterogeneous networks.

Chapter 3

Analysis of Macro-Diversity in LTE-Advanced

3.1 Introduction

In this chapter, we evaluated the soft handover gain in homogeneous deployment environments and mathematical analysis in terms of SINR gain and HO margin between soft handover and hard handover is carried out in a CoMP set.

3GPP Long-Term Evolution (LTE) [7] is based on Orthogonal Frequency Division Multiple Access (OFDMA) technology. One of the main goals of LTE is to provide seamless access to voice and multimedia services with strict latency requirements which is achieved by the current technology. Hard handover is supported for the LTE systems using L3-filter, hysteresis, and time-to-trigger mechanisms [16]. Coordinated Multi-Point (CoMP) transmission / reception is being studied in LTE-A [7] for further evolution of 3GPP LTE. It is foreseen that evolution of backhaul technology

can accommodate increased backhaul requirements of CoMP in LTE-A deployment timeframe. Soft handover is a key technique to extend cell coverage and increase the cell edge user data rate in cellular communication systems [9], [10]. Viterbi et al. [9] derived the effect of soft handoff technique on cell coverage and reverse link capacity in the CDMA system. With soft handoff, a user equipment (UE) in downlink receives signals from multiple BSs. The macro-diversity gain obtained by combining the signals received from multiple BSs may compensate for some effect of fast channel fading and improve the communication quality [11]. K. M. Rege presented an analysis of handoff margin for systems allowing soft handoff in CDMA system and those where only hard handoffs are possible [4]. In [13], hybrid handover method, termed site selection diversity transmission (SSDT) was introduced and the handover gain for OFDM-based broadband system was evaluated. Mihailescu et al. analyzed the behavior of the downlink soft handover and derived the macro-diversity gain in terms of SIR for W-CDMA system citeMihailescu. We extend this study to LTE-A downlink. Our analysis in LTE-A system is based on a simple linear topology with two eNBs in the CoMP set. A semi-static scheduler is assumed for downlink scheduling. The rest of this paper is organized as follows: In Section 3.2, we introduce the concept of CoMP set and the propagation model. In Section 3.3, the model for downlink interference is described. An analysis of handover margins based on the interference analysis described in Section 3.4 and numerical results are presented in Sections 3.5. Finally, conclusions are given in Section 3.6.

3.2 CoMP Models and Assumptions

CoMP is one of the key techniques for LTE-A to improve the coverage and the cell edge user throughput. It is considered as an effective approach for inter-cell interference coordination in LTE-A. In the downlink, CoMP techniques are categorized into two methods: coordinated beamforming and joint transmission [12], [8]. Coordinated beamforming is considered as a simple solution to avoid beam collision with limited coordination among neighboring sites. Inter-site joint transmission is a type of joint processing scheme where user data is shared among the neighboring sites and is jointly processed by multiple sites. Full channel knowledge or precoding matrix is shared among the neighboring sites. In this paper, we focus on the inter-site joint transmission. This section presents the models and assumptions used to evaluate the macro-diversity gain.

3.2.1 CoMP Set

A regular hexagonal 19 cell layout with the reference eNB₀ and 18 neighboring eNBs is assumed in Fig. 3-1. CoMP cooperating set is the set of (geographically separated) points directly or indirectly participating in data transmission to the UE. The CoMP cooperating set may be determined as network-decided CoMP cooperating set or UE-specific CoMP cooperating set [17]. For the simplicity of derivation, we consider two eNBs (eNB₀ and eNB₁) as CoMP transmission points in the cooperating set. CoMP measurement set is the set of cells for which channel state information (CSI) on the link to the UE is reported. CoMP set is applicable to cell edge UEs and this decision

is based on the downlink received signal power.

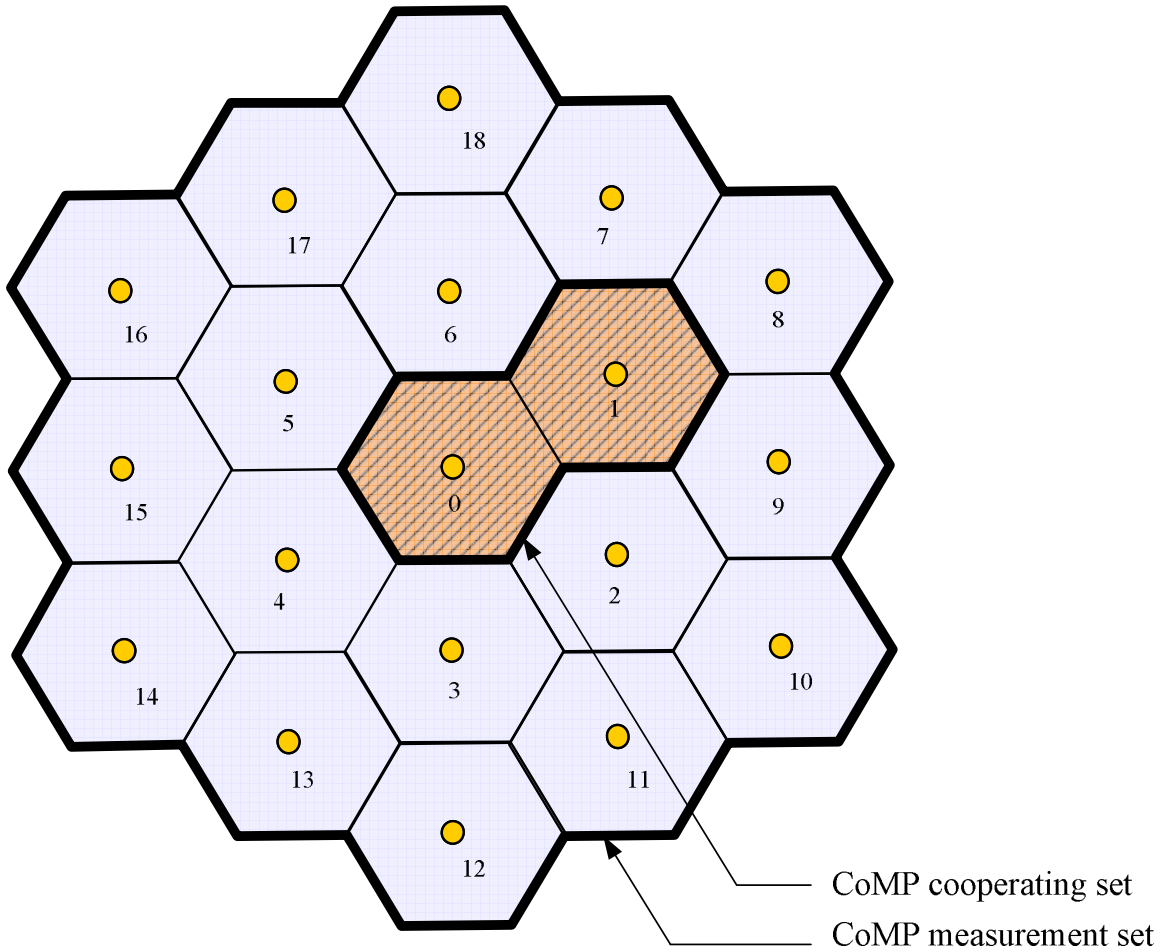


Figure 3-1: CoMP Set.

3.2.2 System Scenario

The propagation loss is generally modeled as the product of the m th power of distance and a log-normal component representing shadowing loss. This shadowing effect is modeled as a log-normal distribution. In this chapter, we only take into account the long-term propagation loss, i.e., pathloss and shadowing. Let us consider a UE

located at a distance r surrounded by 18 cells in the CoMP measurement set. The pathloss between the i -th UE ($i = 0 \dots N$) and an adjacent j -th eNB ($j = 0 \dots C$) is given by

$$L(i, j) = r_{i,j}^{-m} 10^{\xi_{i,j}/10} \quad (3.1)$$

where m is a pathloss exponent, $r_{i,j}$ is the distance between the i -th UE and j -th eNB and $\xi_{i,j}$ is the attenuation in dB due to shadow fading which is modeled as a zero-mean Gaussian random variable with standard deviation σ . Empirical data shows that m is around 4 and σ around 8. Considering the dependence of the shadow fading of different eNBs, $\xi_{i,j}$ is expressed as the weighted sum of a component ξ which is common to all eNBs and a component $\xi_{i,j}$ which is independent from one eNB to another. Both components are assumed to be Gaussian distribution random variables with zero mean and standard deviation σ [9].

Thus, the random component of the received signal at eNB be expressed as $\xi_{i,j} = a\xi + b\xi_{i,j}$ where $a^2 + b^2 = 1$. Note that the shadowing in the received signal depends on the UE environment, the variables $\xi_{i,j}$ and $\xi_{i,l}$ are correlated [10]. Thus, a correlation of coefficient between two eNBs, j and l , defines as

$$\frac{E(\xi_{i,j}, \xi_{i,l})}{\sigma^2} = a^2 = 1 - b^2 \quad (j \neq l) \quad (3.2)$$

We can assume that the near-field and eNB specific propagation uncertainties have equal standard deviation. Therefore $a^2 = b^2 = 0.5$ and the normalized covariance is 0.5 for all pairs of eNBs. We consider defined CoMP transmission points in the

cooperating set where a UE_i on a straight line joining reference eNB_0 and neighboring eNB_1 as shown in Fig. 3-2. The distance between the UE_i and eNB_j will be denoted by $r_{i,j}$ with $j = 0, 1, 2, \dots, C$ whereas $\xi_{i,j}$ will denote the shadow fading exponent for the signal received at that eNB. Assuming both eNBs located on a horizontal axis with angle = 0.

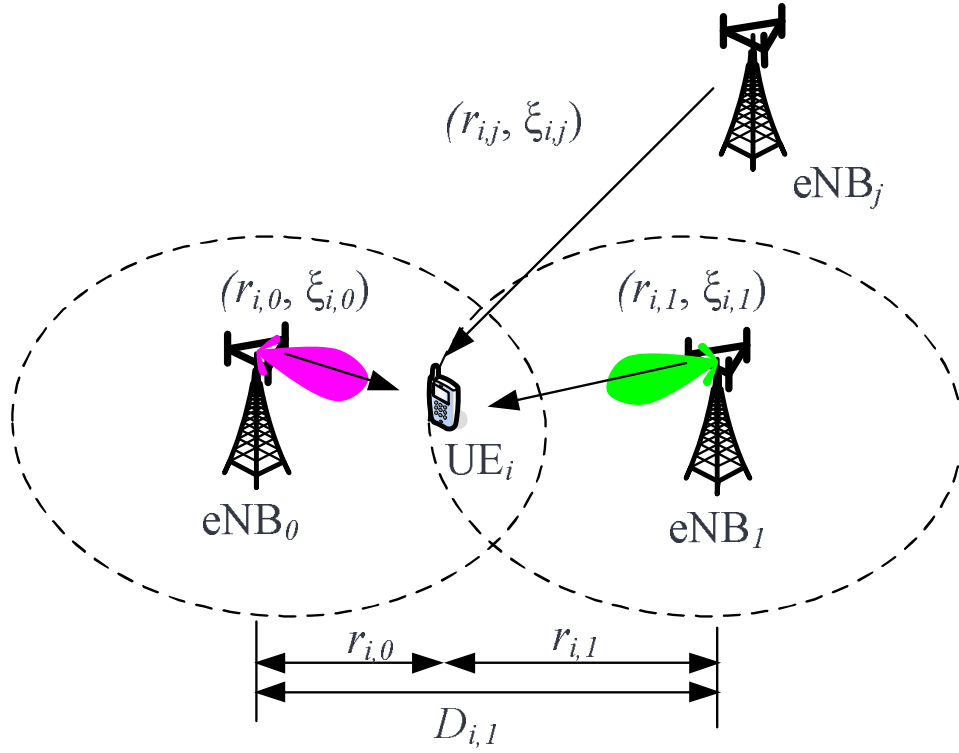


Figure 3-2: System Model.

3.3 Downlink Interference Analysis

To evaluate the SINR, interference modeling is required and a general LTE-A system is used as the target system. The total interference (I_{tot}) experienced by the UE is composed of two parts: Intra-cell (I_{intra}) and inter-cell interference (I_{inter}).

Let $SINR_{i,j}^{user}$ be the SINR measured at UE_i which is connected to eNB_j given by

$$\begin{aligned} SINR_{i,j}^{user} &= \frac{C_{i,j}}{I_{intra_{i,j}} + I_{inter_{i,j}} + N_0} \\ &= \left(\frac{I_{intra_{i,j}}}{C_{i,j}} + \frac{I_{inter_{i,j}}}{C_{i,j}} + \frac{N_0}{C_{i,j}} \right)^{-1} \end{aligned} \quad (3.3)$$

Where N_0 is thermal noise per user including UE noise figure. And $C_{i,j}$ is the power signal received from eNB_j . If we can take expectations from (3.3), we can write Jensen's inequality for convex function as

$$E[SINR_{i,j}^{user}] \geq \left(E\left[\frac{I_{intra_{i,j}}}{C_{i,j}}\right] + E\left[\frac{I_{inter_{i,j}}}{C_{i,j}}\right] + \left[\frac{N_0}{C_{i,j}}\right] \right)^{-1} \quad (3.4)$$

3.3.1 Intra-cell Interference

The intra-cell interference to a certain UE comes from its serving eNB and caused by Inter carrier Interference. Inter carrier Interference is generated from the internal carriers of UE_i and only carriers on the border may impact on neighboring UEs, as shown in Fig. 3-3(a). In this chapter, we only take into consideration small amount of interference by carriers on the border.

The total transmitted power in the downlink for own eNB_0 is given by

$$P_{tot0} = \sum_{i=1}^N P_{i,0} \quad (3.5)$$

With our definition, the amount of intra-cell interference is obtained by

$$I_{intra_{i,0}} = \varepsilon \cdot \delta \cdot \frac{\rho_0 \cdot P_{tot_0}}{N_{tot}} \cdot L(i, 0) \quad (3.6)$$

where $L(i, 0)$ and δ is the pathloss and activity factor respectively. For simplicity we define ε as an intra-cell interference coefficient. We assume Semi-static scheduler is used for UE resource allocation and total transmitted power is equally divided into each UEs by N_{tot} which is defined as the total number of user. Fig. 3-3(a) explains the resource allocation by Semi-Static Scheduler and inter carrier interference distribution for UE_{*i*}. ρ_0 is the fraction of used physical resource blocks (PRBs) in own eNB₀, and defined as

$$\rho_0 = \frac{N_{used}^{PRB}}{N_{tot}^{PRB}} \quad (3.7)$$

Consequently, from (3) and (6), we can obtain

$$\frac{I_{intra_{i,0}}}{C_{i,0}} = \frac{\frac{\varepsilon \cdot \delta \cdot \rho_0 \cdot P_{tot_0} \cdot L(i,0)}{N_{tot}}}{\frac{\rho_0 \cdot P_{tot_0} \cdot L(i,0)}{N_{tot}}} = \varepsilon \cdot \delta \quad (3.8)$$

Note that (8) is a function of the ε and δ . And it is independent from UE location and the number of other UEs. This means that we only need to consider UE_{*i*} (for example, UE₁ in Fig. 3-3(c)) in eNB₀ with these parameters for intra-cell interference analysis.

3.3.2 Inter-cell Interference

To a UE linked to eNB_{*i*}, theoretically the inter-cell interference is the power received by UE from all other eNBs around it except its own serving eNB_{*i*}. Inter-cell interference, with eNB₀ being the reference cell for UE_{*i*}, written as

$$I_{inter_{i,j}} = \delta \cdot \sum_{j=1}^C \frac{\rho_j \cdot P_{tot_j}}{N_{tot}} \cdot L(i, j) \quad (3.9)$$

We assume that all number of users, and the cell loading is equal in all eNBs and all transmitted power to every users in each eNB is also same. Then we can obtain

$$\begin{aligned} \frac{I_{inter_{i,j}}}{C_{i,0}} &= \frac{\delta \cdot \sum_{j=1}^C \rho_j \cdot P_{tot_j} \cdot L(i, j)}{\frac{\rho_0 \cdot P_{tot_0} \cdot L(i, 0)}{N_{tot}}} \\ &= \delta \cdot \frac{\sum_{j=1}^C L(i, j)}{L(i, 0)} \\ &= \delta \cdot \sum_{j=1}^C \left(\frac{r_{i,0}}{r_{i,j}} \right)^m \cdot 10^{(\xi_{i,j} - \xi_{i,0})/10} \end{aligned} \quad (3.10)$$

Fig. 3-3(b) shows the example of User allocation in eNBs. For simplicity we only considered interference from users allocated in the PRBs of UE₁ and others are neglected. With this reason, this system can then be modeled as narrow band interference analysis unlike CDMA/WCDMA system. And Fig. 3-3(c) shows Multi-point reception with interference where we assume that 2 eNBs are selected for CoMP transmission points.

3.4 Analysis of Hard and Soft Handovers

In this section, we analyze the soft handover gain by evaluating the HO gain. The two key design parameters are CoMP set size and the handover (HO) margin. The HO gain also depends on the UE receiver processing. Maximal Ratio Combining (MRC) is assumed in this paper.

3.4.1 Hard Handover Analysis

Note finally that all parameters in (3.10) are UE location dependent and deterministic except δ , $\xi_{i,0}$ and $\xi_{i,j}$, which are random but do not depend on location. Suppose that only a single cell's RSRP is being tracked at any one time, and that handover between cells is performed at the CoMP cooperation set boundary. This is idealized to avoid "ping-pong" effect and this condition may be alleviated by requiring handovers to occur only when the second cell's RSRP is sufficiently above that of the first. We define

$$M_{i,j} = 10mlogr_{i,j} \quad (3.11)$$

and we can derive the probability P_0 that UE_{*i*} is only anchored to the eNB₀ as

$$\begin{aligned} P_0 &= Prob[RSRP_0 > RSRP_1 + M_{SH}] \\ &= Q\left(\frac{M_{i,0} - M_{i,1} + M_{SH}}{\sqrt{2}b\sigma}\right) \end{aligned} \quad (3.12)$$

M_{SH} is the soft handover margin and if it is 0, then it is hard handover. Q is defined as

$$Q(x) = \frac{1}{\sqrt{2\pi}} \int_x^{\infty} \exp^{-z^2/2} dz \quad (3.13)$$

In order to calculate $E[SINR_{i,0}^{user}]$ without macrodiversity using (3.8), we have

$$\frac{I_{intra_{i,0}}}{C_{i,0}} = E \left[\frac{I_{intra_{i,0}}}{C_{i,0}} \right] = \varepsilon \cdot \delta \quad (3.14)$$

From (3.10), we can obtain

$$\begin{aligned} E \left[\frac{I_{inter_{i,j}}}{C_{i,0}} \right] &= \delta \cdot \sum_{j=1}^C \left(\frac{r_{i,0}}{r_{i,j}} \right)^m \cdot E[10^{(\xi_{i,j} - \xi_{i,0})/10}; \\ &\quad RSRP_0 > RSRP_1 + M_{SH}] \\ &= \delta e^{(\beta\sigma)^2/2} \sum_{j=1}^C \left(\frac{r_{i,0}}{r_{i,j}} \right)^m Q \left(\beta\sigma + \frac{M_{i,0} - M_{i,j} + M_{SH}}{\sigma} \right) \end{aligned} \quad (3.15)$$

where we have $\xi_{i,j} - \xi_{i,0} = b(\xi_{i,j} - \xi_{i,0})$, which is a Gaussian random variable with zero mean and independent. And $\beta = \ln(10)/10$.

Using (3.14) and (3.15), the $E[SINR_{i,0}^{user}]$ for UE_{*i*} anchored only at eNB₀ can be calculated from (3.4). Similarly, the P_1 and the $E[SINR_{i,1}^{user}]$ for UE_{*i*} anchored only at eNB₁ can be derived from same formula.

3.4.2 Soft Handover Analysis

With 2-way SHO, desired signal from the two active eNBs in CoMP are combined together while the rest of the eNBs are considered interferences. Maximal ratio com-

binning is considered in this chapter.

We can derive the Probability P_{01} when the UE_i is connected to 2 eNBs simultaneously in the CoMP cooperating set as

$$\begin{aligned}
P_{01} &= Prob(RSRP_1 - M_{SH} < RSRP_0 < RSRP_1 + M_{SH}) \\
&= Q\left(\frac{M_{i,0} - M_{i,1} - M_{SH}}{\sqrt{2}b\sigma}\right) - Q\left(\frac{M_{i,0} - M_{i,1} + M_{SH}}{\sqrt{2}b\sigma}\right) \quad (3.16)
\end{aligned}$$

From (3.10), we can obtain

$$\begin{aligned}
E\left[\frac{I_{inter_{i,j}}}{C_{i,0}}\right] &= \delta \cdot \sum_{j=1}^C \left(\frac{r_{i,0}}{r_{i,j}}\right)^m \cdot E[10^{(\xi_{i,j} - \xi_{i,0})/10}; \\
&\quad RSRP_1 - M_{SH} < RSRP_0 < RSRP_1 + M_{SH}] \\
&+ \delta \cdot \sum_{j=2}^C \left(\frac{r_{i,0}}{r_{i,j}}\right)^m \cdot E[10^{(\xi_{i,j} - \xi_{i,0})/10}; RSRP_0 > RSRP_j + M_{SH}] \quad (3.17)
\end{aligned}$$

Again, (3.16) can be rewritten as

$$\begin{aligned}
E\left[\frac{I_{inter_{i,j}}}{C_{i,0}}\right] &= \delta e^{(\beta\sigma)^2/2} Q\left(\beta\sigma + \frac{M_{i,0} - M_{i,1} - M_{SH}}{\sigma}\right) \\
&- \delta e^{(\beta\sigma)^2/2} Q\left(\beta\sigma + \frac{M_{i,0} - M_{i,1} + M_{SH}}{\sigma}\right) \\
&+ \delta e^{(\beta\sigma)^2/2} \sum_{j=2}^C \left(\frac{r_{i,0}}{r_{i,j}}\right)^m Q\left(\beta\sigma + \frac{M_{i,0} - M_{i,j} + M_{SH}}{\sigma}\right) \quad (3.18)
\end{aligned}$$

Using (3.14) and (3.18), the $\overline{E[SINR_{i,0}^{user}]}$ for UE_i located at handover area can be calculated from (4). Similarly, the $\overline{E[SINR_{i,0}^{user}]}$ can be derived from same formula.

Thus we can obtain $\overline{E[SINR_{i,01}^{user}]}$ with the maximum ratio combining. Finally, the average SINR with macrodiversity is

$$E[SINR_{i,total}^{user}] = P_0 E[SINR_{i,0}^{user}] + P_0 \overline{E[SINR_{i,01}^{user}]} + P_1 E[SINR_{i,1}^{user}] \quad (3.19)$$

3.5 Numerical Results

A mathematical analysis was carried out using the SINR expressions derived in the previous sections. The effect of system parameters on the SINR performance is evaluated for the scenario described in section 3.2.2. Those parameters are:

M_{SH}	soft handover margin
$r_{i,0}/D_{i,1}$	normalized cell distance
δ	activity factor
m	pathloss exponent
σ	standard deviation of shadowing fading (in dB)
ε	intra-cell interference coefficient

In Fig. 3-4, the SINR versus distance $r_{i,0}/D_{i,1}$ for different values of M_{SH} is plotted. We considered activity factor of $\delta = 0.5$ and $m = 3$. The X-axis defines the normalized distance in the range from 0.1 to 0.9, where 0.5 means the cell border. When M_{SH} is varied from 0 to 2 dB, and from 2 dB to 4 dB, the SINR at the cell border is increased by 1.8 dB and 1.2 dB, respectively

Fig. 3-5 shows the SINR when m is increased from 3 to 4. Compared with Fig.

3-4, the result shows that the gain in SINR is about 2 dB. This is due to inter-cell interference reduction due to increased path loss for signals coming from the neighboring cells.

In Fig. 3-6, we show the SINR as the intra-cell interference factor ε is varied. The figure shows that the SINR improves as ε becomes smaller, due to decreased intra-cell interference. The effect of intra-cell interference on SINR is larger for large values of M_{SH} relative to the inter-cell interference, resulting in larger difference in SINR values. It is also observed that the SINR becomes saturated when $M_{SH}=6$ dB.

The factor that mainly affects soft handover performance is the propagation parameters. We evaluate the SINR with respect to the choice of parameters m and σ . Fig. 3-7 shows the effect of pathloss exponent m on the SINR with the soft handover margin of 0 to 10. The SINR increases as the M_{SH} is increased from 0 to 4. The SINR improves significantly when m increases due to inter-cell interference reduction. This behaviour was also observed in Fig. 3-4 and Fig. 3-5.

In Fig. 3-8, the SINR versus M_{SH} is plotted for different values σ . The dynamic range of the SINR changes by 0.5 dB to 2 dB when M_{SH} increases from 0 to 10 dB respectively. It is interesting to note that the SINR with higher M_{SH} is increased considerably as the σ is increased since the large differences of two received signal power leads the higher combining gain.

This result could be applied to system planning, where SINR gain can be achieved by optimizing M_{SH} , depending on propagation condition.

3.6 Conclusion

In this chapter, we have presented a mathematical analysis of macro-diversity gain that can be achieved in the LTE-A system. We have derived intra-cell and inter-cell interference models for LTE-A. A mathematical analysis of SINR gain between soft handover and hard handover is carried out based on the Maximal Ratio Combining reception. The results show that propagation parameters significantly affect the choice of the handover margin and the SINR performance. The results in this paper can be used as a guideline in designing and operating the radio network based on LTE-A technology to improve the cell edge user performance. An analysis of handover gain for multiple deployment scenarios including heterogeneous network will be the subject of future research.

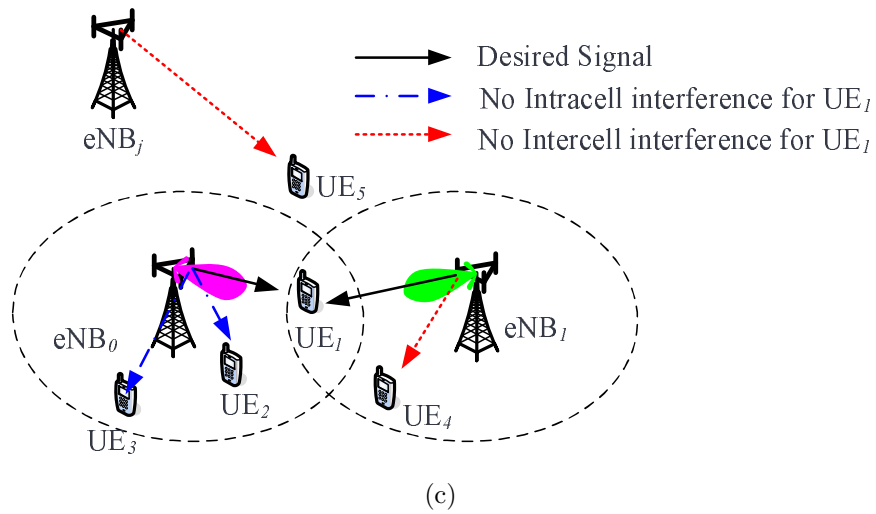
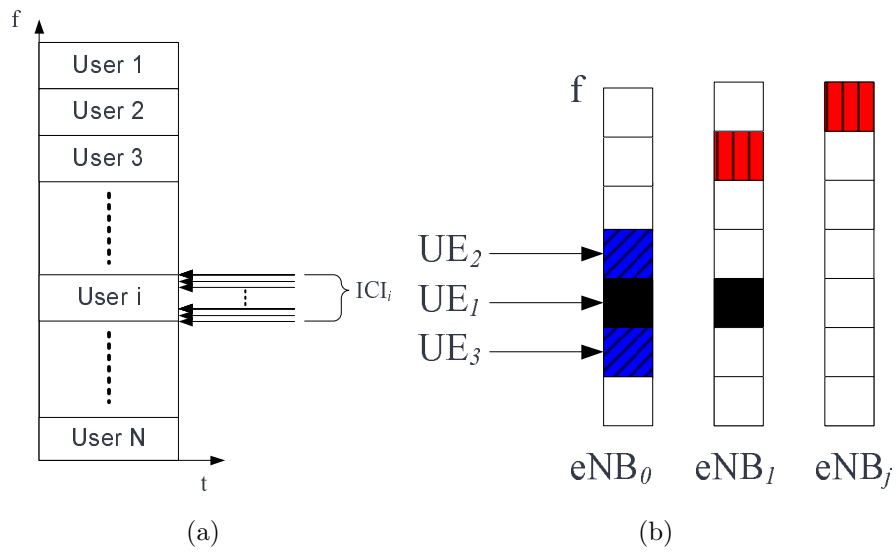


Figure 3-3: Assumption for Interference Analysis (a) Resource allocation by Semi-Static Scheduler (b) Example of User allocation in eNBs and (c) Multi-point reception with interference.

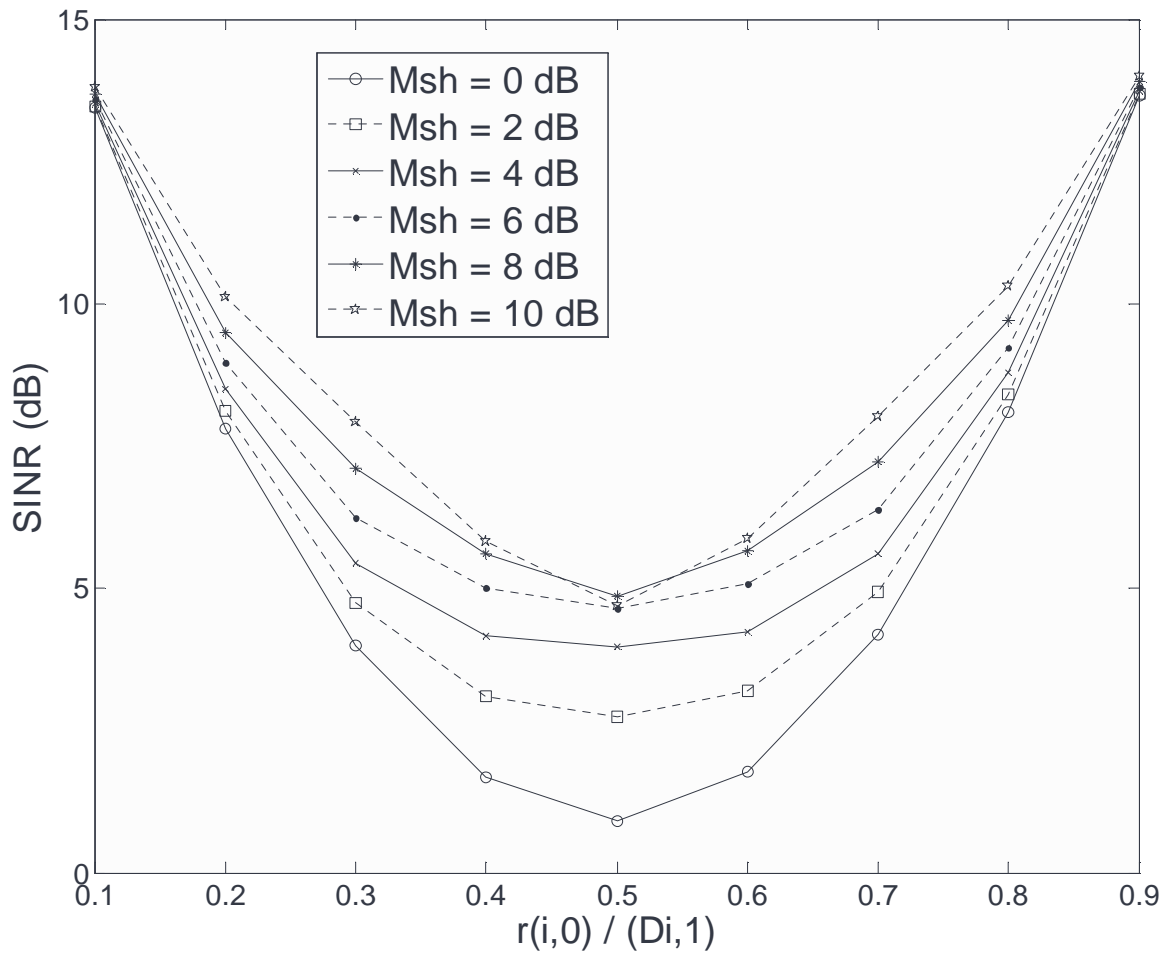


Figure 3-4: SINR depending on distance $r_{i,0}/D_{i,1}$ ($m=3$, $\sigma=8$, and $\varepsilon=0.05$)

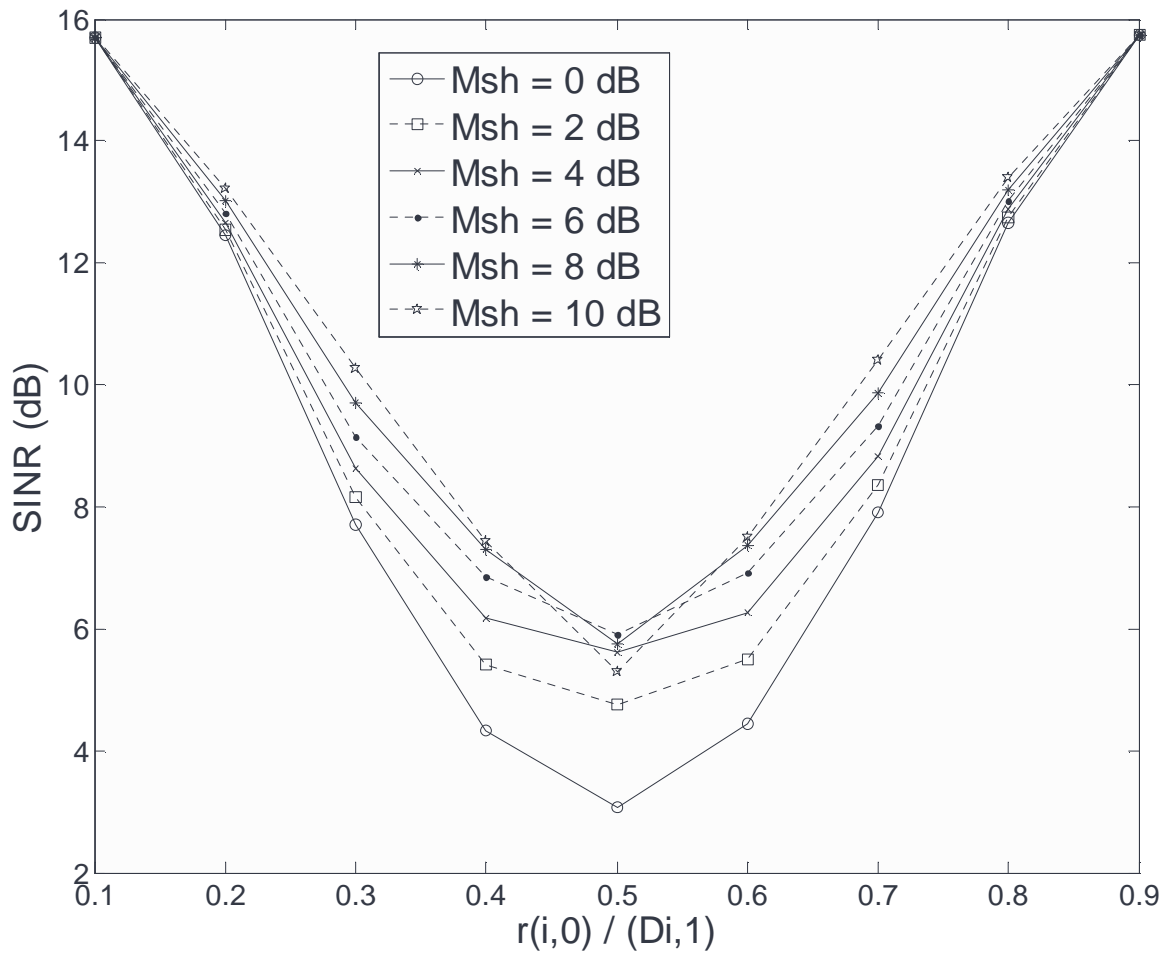


Figure 3-5: SINR depending on distance $r_{i,0}/D_{i,1}$ ($m=4$, $\sigma=8$, and $\varepsilon=0.05$)

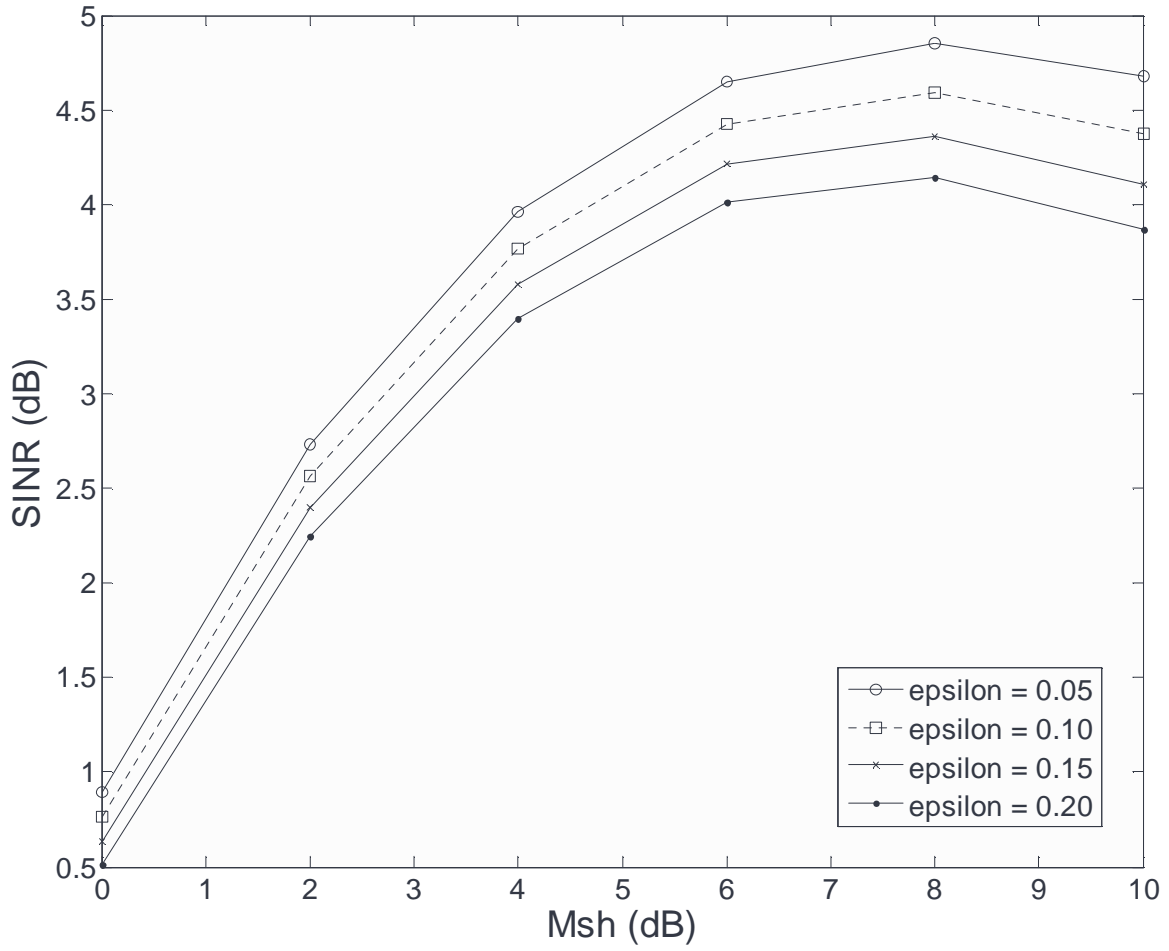


Figure 3-6: SINR versus M_{SH} for different values of ε .

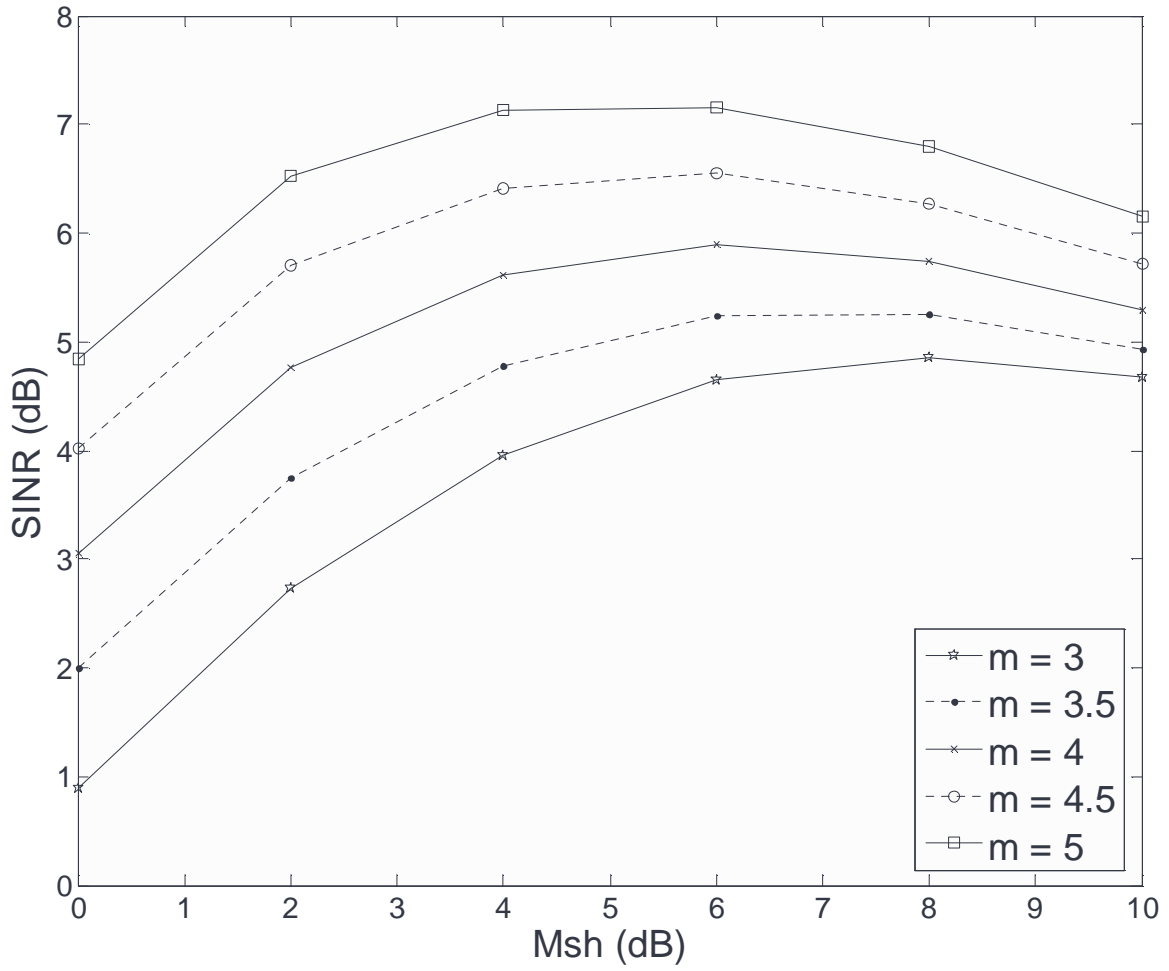


Figure 3-7: SINR versus M_{SH} for different values of pathloss exponent m .

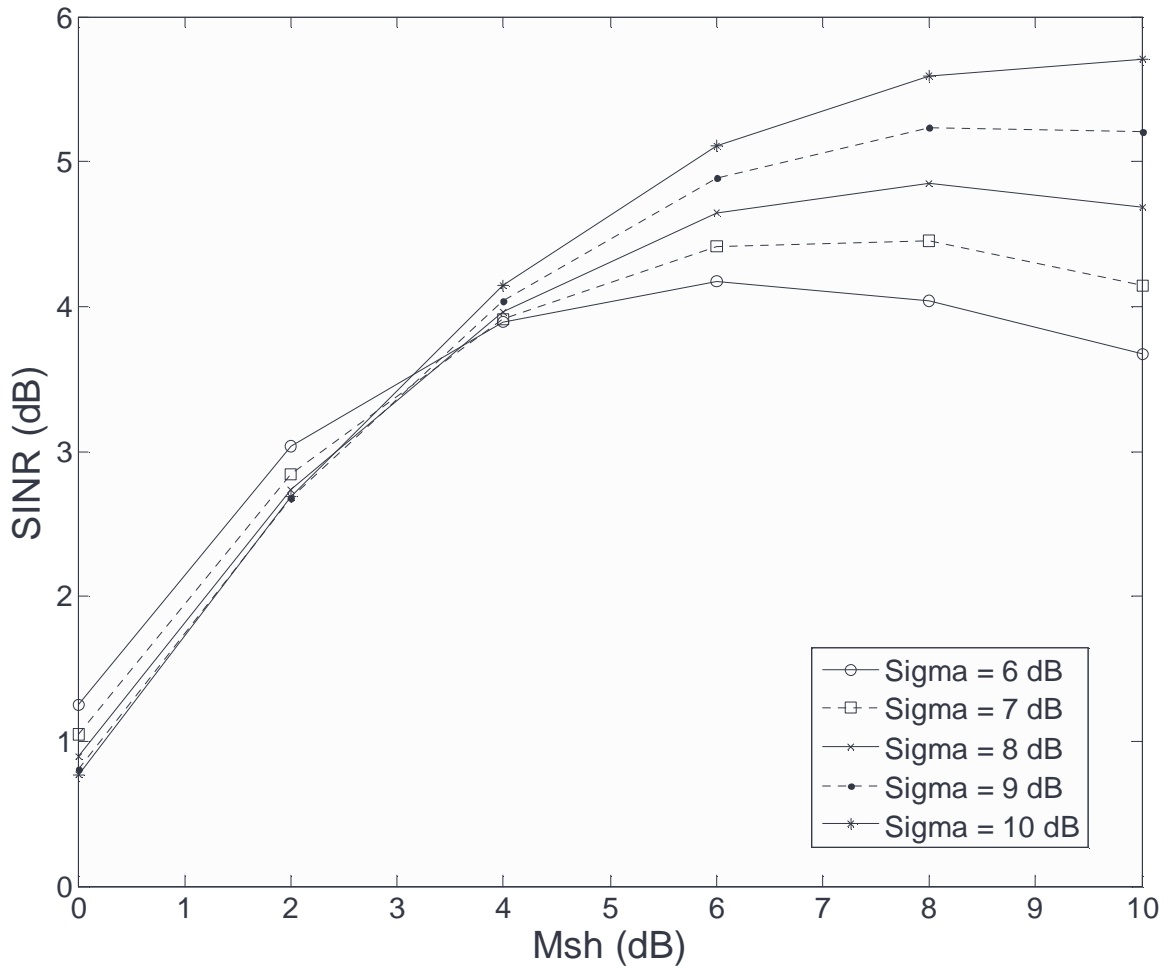


Figure 3-8: SINR versus M_{SH} for different values of σ .

Chapter 4

Optimized Handover for

Heterogeneous Network

Deployment in LTE-Advanced

4.1 Introduction

3GPP Long Term Evolution (LTE) including Release 8 [19] is based on Orthogonal Frequency Division Multiple Access (OFDMA) technology and has been working on various areas to improve spectral efficiency and LTE performance in the framework of LTE-A, which include heterogeneous networks, interference management, carrier aggregation, and higher order MIMO. Given the goals of LTE-A, heterogeneous network configurations have been included in the LTE-A Release 12 study item [20] and three different types of low-power nodes have been defined as mixed deployments consisting of macro, pico and femto and relay nodes. The heterogeneous network deployment is

typically characterized by the types and location of local eNBs deployed in the macro eNB coverage areas [21]. The deployment of macro and pico cell is intended to cover areas with non-homogeneous user distributions in a geographical area of high density of mobile users, and the co-existence of home eNBs (femto) is to support private devices with relatively little control. And relay nodes can be used to extend coverage or to enhance the cell throughput of the macro eNB. In particular, we are interested in the mixed case of macro eNB and pico eNBs in co-channel deployment scenario where the RF coverage areas may be overlapped

Support of heterogeneous network will require the modification of radio link connection approach due to coverage imbalance between the DL and UL by the different transmit powers of macro and pico eNBs. In a conventional network including LTE Release 8, the UE is typically connected to the cell that provides the strongest DL signal power. However, the UE suffers from strong interference due to UL/DL link imbalance in a heterogeneous network.

This UL/DL imbalance is a well-known problem in cellular wireless communication system caused by signal strength imbalances. The differences of UL/DL coverage on a cell boundary triggers sudden UL synchronization losses on some of radio legs of a WCDMA call upon handover. And in the case of an HSUPA call, if the UL synchronization of the radio leg serving the HSDPA leg is lost, it leads throughput stalls. Another problem is that the imbalanced cell is likely to experience abnormal levels of uplink interference which, in turn, can lead to call instability and a high call drop rate when the cell load increases.

Our analysis in LTE-A system is based on a simple linear topology with two eNBs

in the CoMP set. A semi-static scheduler is assumed for downlink scheduling. The rest of this chapter is organized as follows: In Section 4.2, we introduce the concept of CoMP set and the propagation model. We focused on Join processing method. And the model for downlink interference is described including a Macro and a pico cell in a same coverage area.

An analysis of handover margins based on the interference analysis in heterogeneous network configuration described in Section 4.3 and 4.4. Numerical results are presented in Sections 4.5. Finally, conclusions are given in Section 4.6.

4.2 Heterogeneous Network Models and Assumptions

A heterogeneous network in LTE is a network containing network nodes, such as eNBs, with different characteristics such as transmission power and RF coverage area. eNBs with different transmission powers are used to support large and small RF coverage areas. The macro eNB with a large RF coverage is deployed in a planned way for blanket coverage or urban, suburban, or rural areas. The RF coverage areas of heterogeneous network nodes could be placed as shown in Fig. 4-1. And coordinated multi-point (CoMP) transmission/reception is considered for LTE-Advanced as a solution to improve the coverage at the edge of cell and data throughput. Downlink CoMP implies dynamic coordination among multiple geographically separated transmission points. Service cell is defined as cell which transmits PDCCH assignments

and this is the serving cell of Rel-8.

CoMP set can be categorized into Joint Processing (JP) where data is available at each point in CoMP cooperating set and Coordinated Scheduling/Beamforming (CS/CB) where data is only available at serving cell but user scheduling/beamforming decisions are made with coordination among cells corresponding to the CoMP cooperating set. CoMP transmission point is a subset of the CoMP cooperating set. And for JP, can be categorized into Joint Transmission and Dynamic cell selection [24]. In this study, we focus on the inter-site joint transmission where data is transmitted from multiple points at a time via PDSCH. This section presents the models and assumptions used to evaluate the macro-diversity gain.

4.2.1 CoMP Set in Heterogeneous Network

In this study, a cellular hexagonal layout has been considered, where a Macro serving eNB and a Pico eNB are interfered by two tiers of 18 Macro neighboring cells as shown in Fig. 4-1. CoMP measurement set is the set of cells about which channel state/statistical information related to their link to the UE is reported while CoMP cooperating set is the set of points directly or indirectly participating in PDSCH transmission to UE. We defined the Macro serving eNB which includes the Pico eNB in the coverage as a CoMP cooperating set and also defined the two tiers of 18 Macro neighboring cells as a CoMP measurement set.

CoMP cooperating set is the set of (geographically separated) points directly or indirectly participating in PDSCH transmission to UE. For the simplicity of deriva-

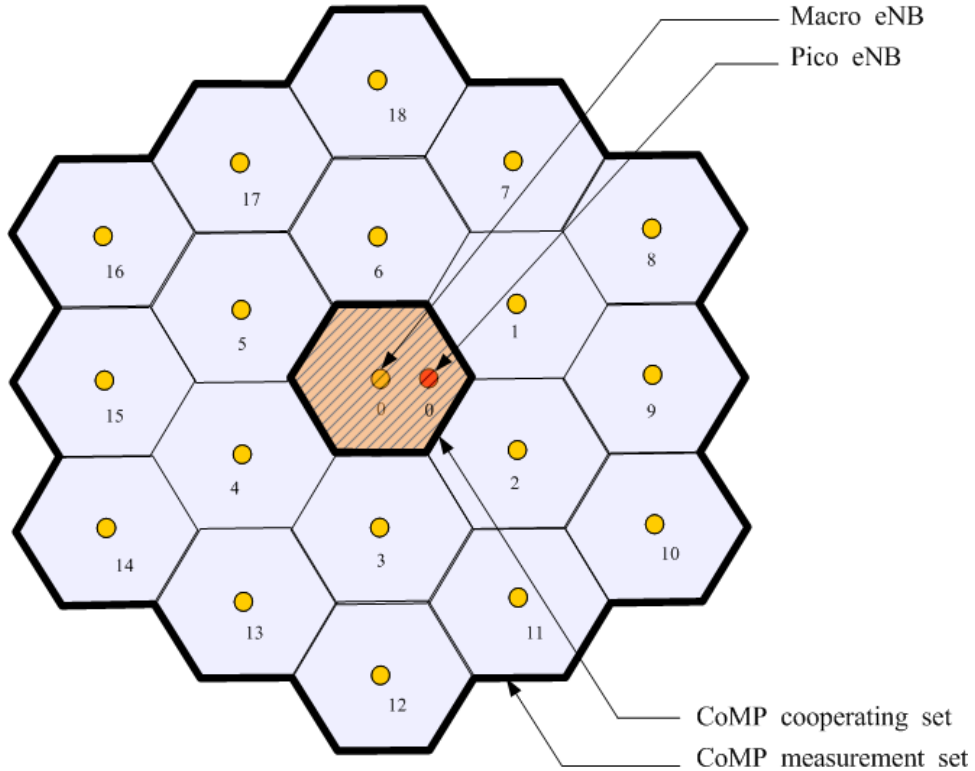


Figure 4-1: Heterogeneous CoMP Set.

tion, we consider two heterogeneous eNBs (Macro eNB and Pico eNB) as CoMP transmission points in the cooperating set. CoMP set is applicable to cell edge UEs and this decision is based on the downlink received signal power.

4.2.2 Propagation Parameters

The propagation loss is generally modeled as the product of the mm -th or pm -th power of distance and a log-normal component representing shadowing loss. This shadowing effect is modeled as a log-normal distribution. In this study, we only take into account the long-term propagation loss, i.e., pathloss and shadowing. Let us consider a UE located at a distance r surrounded by 18 Macro and a Pico cells in

the CoMP measurement set. The pathloss between the i -th UE ($i = 0 \dots N$) and an adjacent Macro j -th eNB $_j^M = (j=0 \dots C)$ defined as $L^M(i, j)$, or a pico k -th eNB $_k^P$ ($k = 0 \dots P$) defined as $L^P(i, k)$ and located in the coverage of the Macro eNB $_{j=0}^M$ is given by

$$L^M(i, j) = r_{i,j}^{-mm} 10^{\xi_{i,j}/10} \quad (4.1)$$

$$L^P(i, k) = r_{i,k}^{-pm} 10^{\xi_{i,k}/10} \quad (4.2)$$

where mm and pm are a pathloss exponent and we defined as a pathloss exponent for Macro and Pico eNB respectively. For the outdoor model of Pico eNB case, the parameter mm and pm are considered in our numerical analysis section 4.5. $r_{i,j}^M$ is the distance between the i -th UE and j -th Macro eNB $_j^M$ and $\xi_{i,j}$ is the attenuation in dB due to shadow fading which is modeled as a zero-mean Gaussian random variable with standard deviation σ . Similarly $r_{i,k}$ is the distance between the i -th UE and k -th Macro eNB $_k^P$ and $\xi_{i,k}$ is the attenuation in dB. We consider only $k=0$ case which means only one Pico eNB. The different parameter values for $\xi_{i,j}$ and $\xi_{i,k}$ are considered in our numerical analysis section 4.5.

Considering the dependence of the shadow fading of heterogeneous eNBs, $\xi_{i,j}$ is expressed as the weighted sum of a component ξ which is common to all eNBs and a component $\xi_{i,j}$ which is independent from one eNB to another. Both components are assumed to be Gaussian distribution random variables with zero mean and standard deviation σ [9].

Thus, the random component of the received signal at eNB be expressed as $\xi_{i,j} =$

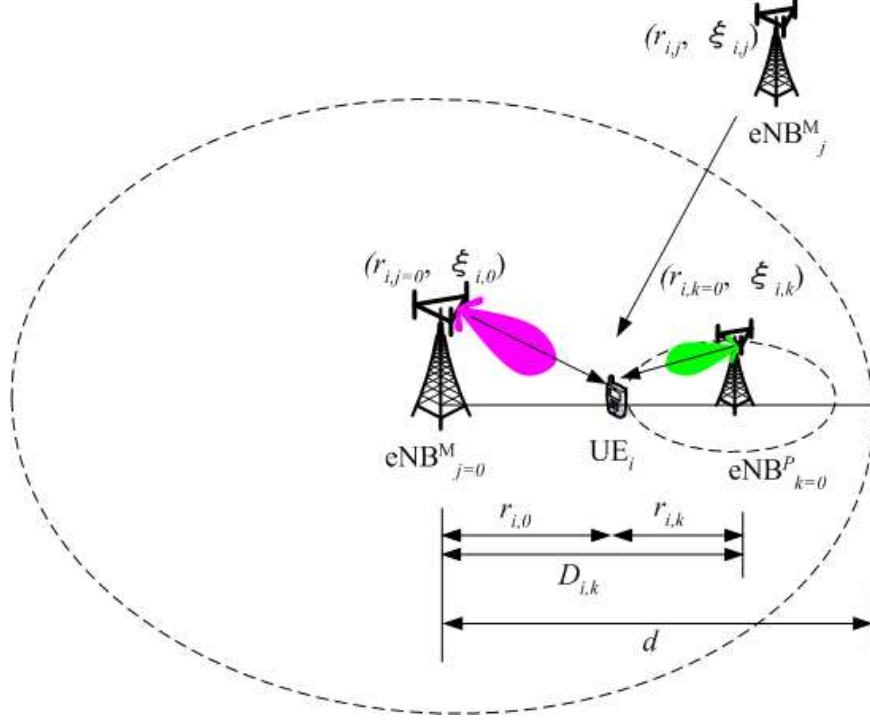


Figure 4-2: System Model.

$a\xi + b\xi_{i,j}$ where $a^2 + b^2 = 1$. Note that the shadowing in the received signal depends on the UE environment, the variables $\xi_{i,j}$ and $\xi_{i,l}$ are correlated [10]. Thus, a correlation of coefficient between two eNBs, j and l , or j and k , defines as

$$E\left(\frac{\xi_{i,j}, \xi_{i,l}}{\sigma^2}\right) = E\left(\frac{\xi_{i,j}, \xi_{i,k}}{\sigma^2}\right) = a^2 = 1 - b^2 \quad (j \neq l, j \neq k) \quad (4.3)$$

We can assume that the near-field and eNB specific propagation uncertainties have equal standard deviation. Therefore $a^2 = b^2 = 0.5$ and the normalized covariance is 0.5 for all pairs of eNBs. We consider defined CoMP transmission points in the cooperating set where a UE_{*i*} on a straight line joining reference Macro eNB_{*j=0*}^{*M*} and neighboring Pico eNB_{*k*}^{*P*} as shown in Fig. 4-2. The distance between the UE_{*i*} and eNB_{*j*}^{*M*} will be denoted by $r_{i,j}$ with $j = 0, 1, 2, \dots, C$ whereas $\xi_{i,j}$ will denote the shadow

fading exponent for the signal received at that eNB. Similarly the distance between the UE_{*i*} and eNB_{*k*}^{*P*} will be denoted by $r_{i,k}$ with $k = 0, 1, 2, \dots, P$.

Assuming both eNBs located on a horizontal axis with angle = 0. The coverage radius of serving Macro eNB₀^{*M*} is defined as d as we want to analysis Handover effect in case of both 'Macro to Pico' and 'Pico to Macro'. And we defined $D_{i,k}^P$ which is sum of $r_{i,0}$ and $r_{i,k}$. In order words, $D_{i,k}^P$ is the Inter-site Distance (ISD) in the heterogeneous deployment scenario.

4.2.3 Power Parameters

Heterogeneous deployments consists of deployments where low power nodes are placed throughout a macro cell layout. The baseline parameters for Transmission power are used for heterogenous network deployment analysis. The baseline for Total BS Tx power $P_{tot_j}^M$ for Macro eNB is proposed by frequency band [24]. We assumed that the frequency band is 10MHz carrier with FDD case which is the most popular system configuration at this moment and the maximum power is 46dBm. The baseline for Pico eNB, we assumed that it is a case of outdoor environment and selected Model 1. Model 1 is based on TR25.814 and IMT.EVAL UMi NLOS Mode while model 2 LOS and NLOS path loss models are based on field measurements. Our numerical results are based on Model 1. For ourdoor Pico case [24], the distance-dependent pathloss from eNB to UE is given by

$$MacrottoUE = 128.1 + 37.6 * \log_{10}(r_{i,j}) \tag{4.4}$$

$$PicotoMacro = 140.7 + 36.7 * \log_{10}(r_{i,k}) \quad (4.5)$$

where $r_{i,j}$ and $r_{i,k}$ are in km and assumed that frequency band is 2GHz. When the heterogeneous network uses different pathloss models, the corresponding pathloss plots for these Macro and Pico eNBs are shown in Fig. 4-3 and Fig. 4-4.

The $P_{tot_j}^M$ for Macro eNB is set to from 46dBm to 19dBm (corresponding $N_{tot_j}^M = 1$ to 10). Similarly the $P_{tot_k}^P$ for Pico eNB is set to from 37dBm to 28dBm (corresponding $N_{tot_k}^P = 1$ to 4). We assumed that the fraction of used physical resource blocks (PRBs) to each UE is different in order to see the effect between PSRP and the Number of User.

The Pathloss in Pico case is larger than the Pathloss in Macro, indicating that the Macro cell can better have SINR performance gain through this propagation model than the Pico can. This results in Fig. 4-3 and Fig. 4-4 show that the RSRP in Macro eNB has a regular higher value by 12 to 13dB under same eNB Power level from 37 to 28dBm due to the different propagation models and the pathloss slopes in it. It is interesting to note that the RSRP level in Pico eNB is relatively low in thier coverage and the RSRP level in Macro eNB is also low if the power level goes down with more users. Choosing a right HO margin with this information will be further investigated in the later Section 4.5

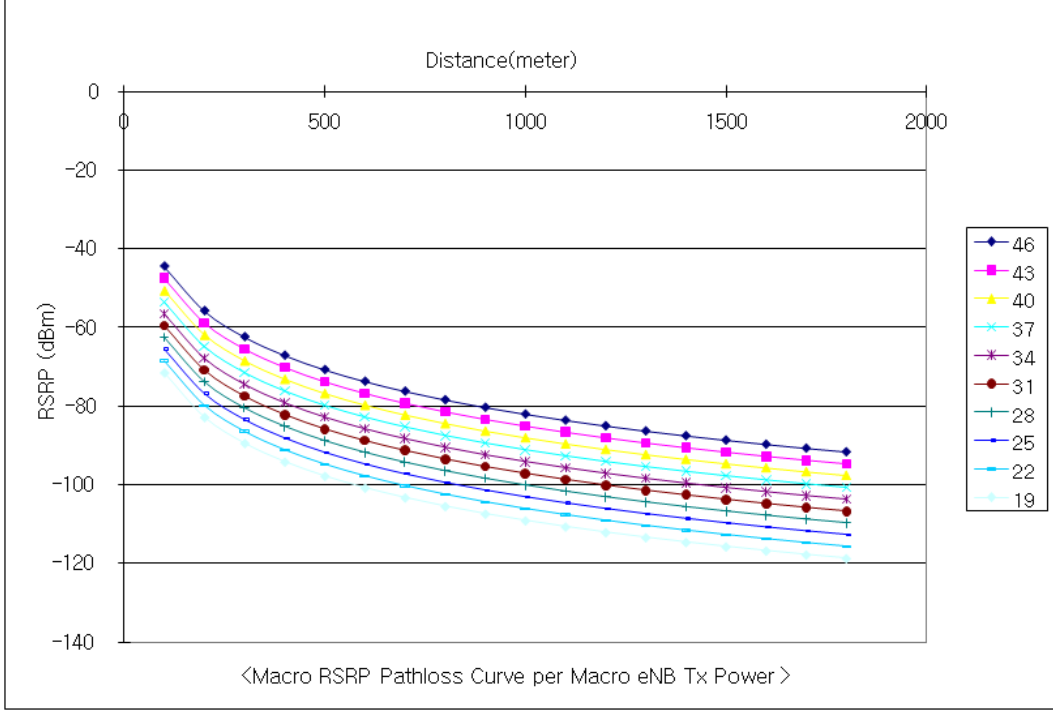


Figure 4-3: Macro eNB RSRP and Pathloss Curve.

4.3 Downlink Interference Analysis in Heterogeneous Network

To evaluate the SINR, interference modeling is required and a general LTE-A system is used as the target system. The total interference (I_{tot}) experienced by the UE is composed of two parts: Intra-cell (I_{intra}) and inter-cell interference (I_{inter}).

Let $SINR_{i,j}^M$ in Macro eNB be the SINR measured at UE_i which is connected to eNB_j^M given by

$$\begin{aligned}
 SINR_{i,j}^M &= \frac{C_{i,j}^M}{I_{intra,i,j}^M + I_{inter,i,j}^M + N_0} \\
 &= \left(\frac{I_{intra,i,j}^M}{C_{i,j}^M} + \frac{I_{inter,i,j}^M}{C_{i,j}^M} + \frac{N_0}{C_{i,j}^M} \right)^{-1}
 \end{aligned} \tag{4.6}$$

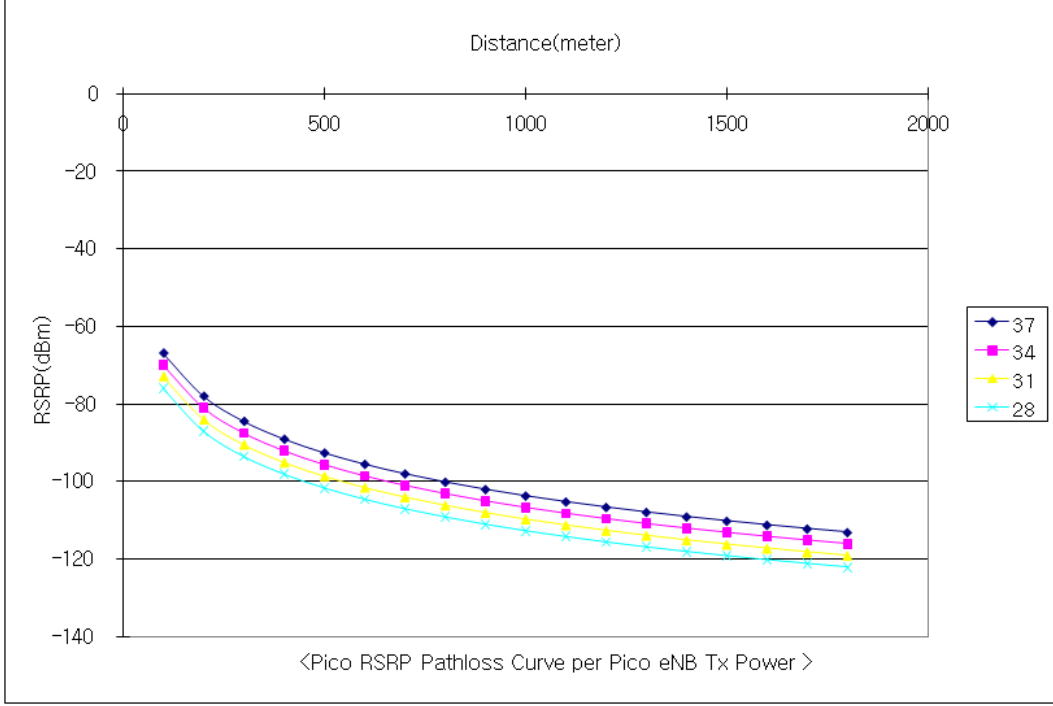


Figure 4-4: Pico eNB RSRP and Pathloss Curve.

Where N_0 is thermal noise per user including UE noise figure. And $C_{i,j}^M$ is the power signal received from eNB $_j^M$. If we can take expectations from (4.6), we can write Jensen's inequality for convex function as

$$E[SINR_{i,j}^M] \geq \left(E\left[\frac{I_{intra,i,j}^M}{C_{i,j}^M}\right] + E\left[\frac{I_{inter,i,j}^M}{C_{i,j}^M}\right] + \left[\frac{N_0}{C_{i,j}^M}\right] \right)^{-1} \quad (4.7)$$

Similarly we can derive the $E[SINR_{i,k}^P]$ which is for Pico eNB.

4.3.1 Intra-cell Interference in Heterogeneous Network

The intra-cell interference to a certain UE comes from its serving eNB and caused by Inter carrier Interference. Inter carrier Interference is generated from the internal carriers of UE $_i$ and only carriers on the border may impact on neighboring UEs. In

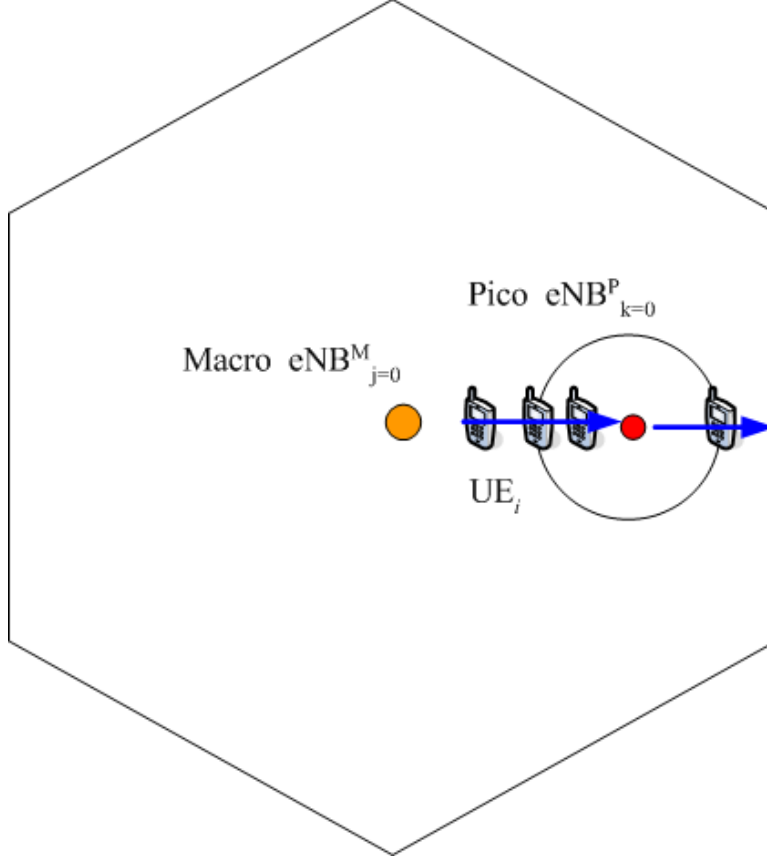


Figure 4-5: Pico and eNB placement and scenario.

this study, we only take into consideration small amount of interference by carriers on the border.

We define $P_{totj=0}^M$ as the total transmitted power of Macro serving ($j = 0$) eNB in the downlink. With this definition, the amount of intra-cell interference in Macro serving eNB is obtained by

$$I_{intra,i,j=0}^M = \varepsilon \cdot \delta \cdot \frac{\rho_{j=0}^M \cdot P_{totj=0}^M}{N_{totj=0}^M} \cdot L^M(i, j = 0) \quad (4.8)$$

where $L^M(i, j = 0)$ and δ is the pathloss and activity factor in Macro serving eNB respectively. For simplicity we define ε as an intra-cell interference coefficient. We

assume Semi-static scheduler is used for UE resource allocation and total transmitted power is equally divided into each UEs by $N_{totj=0}^M$ which is defined as the total number of user in the Macro serving eNB. $\rho_{j=0}^M$ is the fraction of used PRBs in serving eNB $_{j=0}^M$, and defined as

$$\rho_{j=0}^M = \frac{N_{UsedPRBj=0}^M}{N_{TotPRBj=0}^M} \quad (4.9)$$

Consequently, from (4.6) and (4.9), we can obtain

$$\left[\frac{I_{intra,i,j=0}^M}{C_{i,j=0}^M} \right] = \frac{\frac{\varepsilon \cdot \delta \cdot \rho_{j=0}^M \cdot P_{totj=0}^M \cdot L^M(i,j=0)}{N_{totj=0}^M}}{\frac{\rho_{j=0}^M \cdot P_{totj=0}^M \cdot L^M(i,j=0)}{N_{totj=0}^M}} = \varepsilon \cdot \delta \quad (4.10)$$

Note that (4.10) is a function of the ε and δ . And it is independent from UE location and the number of other UEs. This means that we only need to consider UE $_i$ in eNB $_{j=0}^M$ with these parameters for intra-cell interference analysis. Similarly we can derive the interference $I_{intra,i,k=0}^P$ in Pico eNB and also obtain

$$\left[\frac{I_{intra,i,k=0}^P}{C_{i,k=0}^P} \right] = \varepsilon \cdot \delta \quad (4.11)$$

Please note that there is no difference in results of Intra interference analysis.

4.3.2 Inter-cell Interference in Heterogeneous Network

Here we consider two scenarios where a UE is connected to the Macro serving eNB or connected to the Pico eNB. In the former case, the interference comes from the neighboring Macro eNBs and the Pico eNB, and in the latter case, the interference come from all Macro eNBs including the Macro serving eNB. To a UE linked to

eNB $_{j=0}^M$, theoretically the inter-cell interference in Heterogeneous Network is the power received by UE from all other eNBs around it except its own serving eNB $_{j=0}^M$ and the Pico eNB $_{k=0}^P$. Inter-cell interference, with eNB $_{j=0}^M$ being the reference cell for UE $_i$, is obtained as

$$\begin{aligned}
I_{inter_{i,j=0}}^M &= I_{inter_{i,k}}^P + I_{inter_{i,j}}^M \\
&= \delta \cdot \sum_{k=0}^P \rho_{k=0}^P \cdot P_{tot_{k=0}}^P \cdot L^P(i, k=0) \\
&\quad + \delta \cdot \sum_{j=1}^C \rho_j^M \cdot P_{tot_j}^M \cdot L^M(i, j)
\end{aligned} \tag{4.12}$$

We assumed that δ , activity factor for Macro and Pico eNB in Heterogeneous Network is same. However all other parameters are presented for Macro and Pico cases respectively. We differently presented ρ which is the fraction of user PRBs, $\frac{P_{tot}}{N_{tot}}$ which is the Total eNB power allocated to UEs in the coverage, pathloss L and standard deviation σ as follows;

$$\begin{aligned}
\frac{I_{inter_{i,j}}^M}{C_{i,j=0}^M} &= \frac{I_{inter_{i,k=0}}^P}{C_{i,j=0}^M} + \frac{I_{inter_{i,j}}^M}{C_{i,j=0}^M} \\
&= \frac{\delta \cdot \sum_{k=0}^P \rho_{k=0}^P \cdot P_{tot_{k=0}}^P \cdot L^P(i, k=0)}{\rho_{j=0}^M \cdot \frac{P_{tot_{j=0}}^M}{N_{tot_{j=0}}^M} \cdot L^M(i, j=0)} + \frac{\delta \cdot \sum_{j=1}^C \rho_j^M \cdot P_{tot_j}^M \cdot L^M(i, j)}{\rho_{j=0}^M \cdot P_{tot_{j=0}}^M \cdot L^M(i, j=0)} \\
&= \delta \cdot \frac{\rho_{k=0}^P}{\rho_{j=0}^M} \cdot \frac{P_{tot_{k=0}}^P}{\frac{P_{tot_{j=0}}^M}{N_{tot_{j=0}}^M}} \cdot \sum_{k=0}^P \left(\frac{r_{i,j=0}^{mm}}{r_{i,k=0}^{pm}} \right) \cdot 10^{(\xi_{i,k=0} - \xi_{i,j=0})/10} \\
&\quad + \delta \cdot \frac{\rho_j^M}{\rho_{j=0}^M} \cdot \frac{P_{tot_j}^M}{\frac{P_{tot_{j=0}}^M}{N_{tot_{j=0}}^M}} \cdot \sum_{j=1}^C \left(\frac{r_{i,j=0}^{mm}}{r_{i,j}^{mm}} \right) \cdot 10^{(\xi_{i,j} - \xi_{i,j=0})/10}
\end{aligned} \tag{4.13}$$

To a UE linked to eNB $_{k=0}^P$, theoretically the inter-cell interference in Heterogeneous

Network is the power received by UE from all other Macro eNBs around since we placed only one Pico in the scenario. Inter-cell interference, with eNB_{k=0}^P being the reference cell for UE_i, is obtained as

$$\begin{aligned}
I_{inter,i,k=0}^P &= I_{inter,i,j}^M \\
&= \delta \cdot \sum_{j=0}^C \rho_j^M \cdot P_{tot_j}^M \cdot L^M(i,j)
\end{aligned} \tag{4.14}$$

Again (4.14) can be rewritten as

$$\begin{aligned}
\frac{I_{inter,i,k=0}^P}{C_{i,k=0}^P} &= \frac{I_{inter,i,j}^M}{C_{i,k=0}^P} \\
&= \frac{\delta \cdot \sum_{j=0}^C \rho_j^M \cdot P_{tot_j}^M \cdot L^M(i,j)}{\rho_{k=0}^P \cdot \frac{P_{tot_{k=0}}^P}{N_{tot_{k=0}}^P} \cdot L^P(i,k=0)} \\
&= \delta \cdot \frac{\rho_j^M}{\rho_{k=0}^P} \cdot \frac{P_{tot_j}^M}{\frac{P_{tot_{k=0}}^P}{N_{tot_{k=0}}^P}} \cdot \sum_{j=0}^C \left(\frac{r_{i,k=0}^{pm}}{r_{i,j}^{mm}} \right) \cdot 10^{(\xi_{i,j} - \xi_{i,k=0})/10}
\end{aligned} \tag{4.15}$$

In this study, the Macro eNB_{j=0}^M and the Pico eNB_{k=0}^P are selected for CoMP transmission points and the (4.13) and (4.15) can be used for Multi-point reception with interference to derive the CoMP gain in the later Section.

4.4 Analysis of Hard and Soft Handover in Heterogeneous Network

In this section, we analyze the Soft Handover gain by evaluating the HO margin.

We use the Macro eNB_{j=0}^M and the Pico eNB_{k=0}^P for CoMP set for the simplicity of

analysis and defined HO gain as a key design parameter in Heterogeneous Network. MRC combining is assumed to analyze the HO gain.

4.4.1 Hard Handover Analysis

Suppose that only a single cell's RSRP is being tracked at any one time, and that handover between cells is performed at the CoMP cooperation set boundary. This is idealized to avoid "ping-pong" effect and this condition may be alleviated by requiring handovers to occur only when the second cell's RSRP is sufficiently above that of the first. We define

$$M_{i,j}^M = \frac{P_{tot_j}^M}{N_{tot_j}^M} - (128.1 + 37.6 * \log_{10}(\frac{r_{i,j}}{1000})) \quad (4.16)$$

$$M_{i,k}^P = \frac{P_{tot_k}^P}{N_{tot_k}^P} - (140.7 + 36.7 * \log_{10}(\frac{r_{i,k}}{1000})) \quad (4.17)$$

In heterogeneous network, the probability $Prob_{j=0}^M$ and $Prob_{k=0}^P$ can be considered differently unlike homogeneous network since the interference level is different respectively. We can derive the probability $Prob_{j=0}^M$ that UE_i is only anchored to the Macro serving eNB_{j=0}^M as

$$\begin{aligned} Prob_{j=0}^M &= Prob [RSRP_{j=0}^M > RSRP_{k=0}^P + M_{SH}] \\ &= Q \left(\frac{M_{i,j=0}^M - M_{i,k=0}^P + M_{SH}}{\sqrt{2}b\sigma} \right) \end{aligned} \quad (4.18)$$

M_{SH} is the soft handover margin and if it is 0, then it is hard handover. Q is

defined as

$$Q(x) = \frac{1}{\sqrt{2\pi}} \int_x^\infty \exp^{-z^2/2} dz \quad (4.19)$$

In order to calculate $E[SINR_{i,j=0}^M]$ without macrodiversity using (4.10), we have

$$\frac{I_{intra_{i,j=0}}^M}{C_{i,j=0}^M} = E \left[\frac{I_{intra_{i,j=0}}^M}{C_{i,j=0}^M} \right] = \varepsilon \cdot \delta \quad (4.20)$$

From (4.13), we can obtain

$$\begin{aligned} E \left[\frac{I_{inter_{i,j}}^M}{C_{i,j=0}^M} \right] &= \delta \cdot \frac{\rho_{k=0}^P}{\rho_{j=0}^M} \cdot \frac{P_{tot_{k=0}}^P}{\frac{P_{tot_{j=0}}^M}{N_{tot_{j=0}}^M}} \cdot \sum_{k=0}^P \left(\frac{r_{i,j=0}^{mm}}{r_{i,k=0}^{pm}} \right) \cdot E[10^{(\xi_{i,k=0} - \xi_{i,j=0})/10}; \\ &\quad RSRP_{j=0}^M > RSRP_{k=0}^P + M_{SH}] \\ &+ \delta \cdot \frac{\rho_j^M}{\rho_{j=0}^M} \cdot \frac{P_{tot_j}^M}{\frac{P_{tot_{j=0}}^M}{N_{tot_{j=0}}^M}} \cdot \sum_{j=1}^C \left(\frac{r_{i,j=0}^{mm}}{r_{i,j}^{mm}} \right) \cdot E[10^{(\xi_{i,j} - \xi_{i,j=0})/10}; \\ &\quad RSRP_{j=0}^M > RSRP_{k=0}^P + M_{SH}] \\ &= \delta \cdot e^{(\beta\sigma)^2/2} \cdot \frac{\rho_{k=0}^P}{\rho_{j=0}^M} \cdot \sum_{k=0}^P \left(\frac{r_{i,j=0}^{mm}}{r_{i,k=0}^{pm}} \right) Q \left(\beta\sigma + \frac{M_{i,j=0}^M - M_{i,k=0}^P + M_{SH}}{\sigma} \right) \\ &+ \delta \cdot e^{(\beta\sigma)^2/2} \cdot \frac{\rho_j^M}{\rho_{j=0}^M} \cdot \sum_{j=1}^C \left(\frac{r_{i,j=0}^{mm}}{r_{i,j}^{mm}} \right) Q \left(\beta\sigma + \frac{M_{i,j=0}^M - M_{i,j}^P + M_{SH}}{\sigma} \right) \end{aligned} \quad (4.21)$$

and also we can derive the probability $Prob_{k=0}^P$ that UE_i is only anchored to the

Pico $eNB_{k=0}^P$ as

$$\begin{aligned}
Prob_{k=0}^P &= Prob [RSRP_{k=0}^P > RSRP_{j=0}^M + M_{SH}] \\
&= Q \left(\frac{M_{i,k=0}^P - M_{i,j=0}^M + M_{SH}}{\sqrt{2}b\sigma} \right)
\end{aligned} \tag{4.22}$$

In order to calculate $E[SINR_{i,k=0}^P]$ without macrodiversity, we can use (4.11).

And from (4.15), we can obtain

$$\begin{aligned}
E \left[\frac{I_{inter,i,j}^M}{C_{i,k=0}^P} \right] &= \delta \cdot \frac{\rho_j^M}{\rho_{k=0}^P} \cdot \frac{P_{totj}^M}{\frac{P_{totk=0}^P}{N_{totk=0}^P}} \cdot \sum_{j=0}^C \left(\frac{r_{i,k=0}^{pm}}{r_{i,j}^{mm}} \right) \cdot E[10^{(\xi_{i,j} - \xi_{i,k=0})/10}, \\
&\quad RSRP_{k=0}^P > RSRP_j^M + M_{SH}] \\
&= \delta \cdot e^{(\beta\sigma)^2/2} \cdot \frac{\rho_j^M}{\rho_{k=0}^P} \cdot \sum_{j=0}^C \left(\frac{r_{i,k=0}^{pm}}{r_{i,j}^{mm}} \right) Q \left(\beta\sigma + \frac{M_{i,k=0}^P - M_{i,j}^M + M_{SH}}{\sigma} \right)
\end{aligned} \tag{4.23}$$

where we have $\xi_{i,j} - \xi_{i,j=0} = b(\xi_{i,j} - \xi_{i,j=0})$ and $\xi_{i,j} - \xi_{i,k=0} = b(\xi_{i,j} - \xi_{i,k=0})$, which is a Gaussian random variable with zero mean and independent. And $\beta = \ln(10)/10$ in common.

Using (4.20) and (4.21), the $E[SINR_{i,j=0}^M]$ for UE_i anchored only at eNB_{j=0}^M can be calculated from (4.7). We can also derive the $E[SINR_{i,k=0}^P]$ for UE_i anchored only at eNB_{k=0}^P using (4.11) and (4.23) from same formula.

4.4.2 Soft Handover Analysis

With 2-way SHO, desired signal from the two active eNBs (eNB_{j=0}^M, eNB_{k=0}^P) in CoMP set are combined together while the rest of the eNBs are considered interferences.

Maximal ratio combining is considered in this chapter.

We can derive the Probability $Prob_{j&k=0}^{M\&P}$ when the UE_i is connected to 2 eNBs simultaneously in the CoMP cooperating set as

$$\begin{aligned}
Prob_{j&k=0}^{M\&P} &= Prob(RSRP_{k=0}^P - M_{SH} < RSRP_{j=0}^M < RSRP_{k=0}^P + M_{SH}) \\
&= Q\left(\frac{M_{i,j=0}^M - M_{i,k=0}^P - M_{SH}}{\sqrt{2}b\sigma}\right) - Q\left(\frac{M_{i,j=0}^M - M_{i,k=0}^P + M_{SH}}{\sqrt{2}b\sigma}\right)
\end{aligned} \tag{4.24}$$

From (4.13), we can obtain the Inter frequency for the Macro eNB as

$$\begin{aligned}
E\left[\frac{I_{inter_{i,j\&k}}^M}{C_{i,j=0}^M}\right] &= \delta \cdot \frac{\rho_{k=0}^P}{\rho_{j=0}^M} \cdot \frac{\frac{P_{tot_{k=0}}^{PP}}{N_{tot_{k=0}}^P}}{\frac{P_{tot_{j=0}}^{PM}}{N_{tot_{j=0}}^M}} \cdot \sum_{k=0}^P \left(\frac{r_{i,j=0}^{mm}}{r_{i,k=0}^{pm}}\right) \cdot E[10^{(\xi_{i,k=0} - \xi_{i,j=0})/10}; \\
&\quad RSRP_{k=0}^P - M_{SH} < RSRP_{j=0}^M < RSRP_{k=0}^P + M_{SH}] \\
&+ \delta \cdot \frac{\rho_j^M}{\rho_{j=0}^M} \cdot \frac{P_{tot_j}^M}{\frac{P_{tot_{j=0}}^{PM}}{N_{tot_{j=0}}^M}} \cdot \sum_{j=1}^C \left(\frac{r_{i,j=0}^{mm}}{r_{i,j}^{mm}}\right) \cdot E[10^{(\xi_{i,j} - \xi_{i,j=0})/10}; \\
&\quad RSRP_{j=0}^M > RSRP_j^M + M_{SH}]
\end{aligned} \tag{4.25}$$

Again, (4.25) can be rewritten as

$$\begin{aligned}
E\left[\frac{I_{inter_{i,j\&k}}^M}{C_{i,j=0}^M}\right] &= \delta \cdot \frac{\rho_{k=0}^P}{\rho_{j=0}^M} \cdot e^{(\beta\sigma)^2/2} \cdot Q\left(\beta\sigma + \frac{M_{i,j=0}^M - M_{i,k=0}^P - M_{SH}}{\sigma}\right) \\
&+ \delta \cdot \frac{\rho_{k=0}^P}{\rho_{j=0}^M} \cdot e^{(\beta\sigma)^2/2} \cdot Q\left(\beta\sigma + \frac{M_{i,j=0}^M - M_{i,k=0}^P + M_{SH}}{\sigma}\right) \\
&+ \delta \cdot \frac{\rho_j^M}{\rho_{j=0}^M} \cdot e^{(\beta\sigma)^2/2} \cdot \sum_{j=1}^C \left(\frac{r_{i,j=0}^{mm}}{r_{i,j}^{mm}}\right) \cdot Q\left(\beta\sigma + \frac{M_{i,j=0}^M - M_{i,j}^M + M_{SH}}{\sigma}\right)
\end{aligned} \tag{4.26}$$

And similarly from (4.13), we can obtain the Inter frequency for the Pico eNB as

$$\begin{aligned}
E \left[\frac{I_{inter_{i,j\&k}}^M}{C_{i,k=0}^P} \right] &= \delta \cdot \frac{\rho_{j=0}^M}{\rho_{k=0}^P} \cdot \frac{P_{tot_{j=0}}^M}{N_{tot_{j=0}}^M} \cdot \sum_{k=0}^P \left(\frac{r_{i,k=0}^{pm}}{r_{i,j=0}^{mm}} \right) \cdot E[10^{(\xi_{i,j=0}-\xi_{i,k=0})/10}; \\
&\quad RSRP_{j=0}^M - M_{SH} < RSRP_{k=0}^P < RSRP_{j=0}^M + M_{SH}] \\
&+ \delta \cdot \frac{\rho_j^M}{\rho_{k=0}^P} \cdot \frac{P_{tot_j}^M}{N_{tot_{k=0}}^P} \cdot \sum_{j=1}^C \left(\frac{r_{i,k=0}^{pm}}{r_{i,j}^{mm}} \right) \cdot E[10^{(\xi_{i,j}-\xi_{i,k=0})/10}; \\
&\quad RSRP_{k=0}^P > RSRP_j^M + M_{SH}]
\end{aligned} \tag{4.27}$$

Again, (4.27) can be rewritten as

$$\begin{aligned}
E \left[\frac{I_{inter_{i,j\&k}}^M}{C_{i,k=0}^P} \right] &= \delta \cdot \frac{\rho_{j=0}^M}{\rho_{k=0}^P} \cdot e^{(\beta\sigma)^2/2} \cdot Q \left(\beta\sigma + \frac{M_{i,k=0}^P - M_{i,j=0}^M - M_{SH}}{\sigma} \right) \\
&- \delta \cdot \frac{\rho_{j=0}^M}{\rho_{k=0}^P} \cdot e^{(\beta\sigma)^2/2} \cdot Q \left(\beta\sigma + \frac{M_{i,k=0}^P - M_{i,j=0}^M + M_{SH}}{\sigma} \right) \\
&+ \delta \cdot \frac{\rho_j^M}{\rho_{k=0}^P} \cdot e^{(\beta\sigma)^2/2} \cdot \sum_{j=1}^C \left(\frac{r_{i,k=0}^{pm}}{r_{i,j}^{mm}} \right) \cdot Q \left(\beta\sigma + \frac{M_{i,k=0}^P - M_{i,j}^M + M_{SH}}{\sigma} \right)
\end{aligned} \tag{4.28}$$

Using (4.20) and (4.26), the $E[SINR_{i,j=0}^M]$ for UE_i located at handover area can be calculated from (4.7). Similarly, the $E[SINR_{i,k=0}^P]$ can be derived from same formula (4.20) and (4.28). Thus we can obtain $E[SINR_{i,j\&k=0}^{M\&P}]$ with the maximum ratio combining. Finally, the average SINR with macrodiversity is

$$E[SINR_{Total}] = Prob_{j=0}^M \cdot E[SINR_{i,j=0}^M] + Prob_{j\&k=0}^{M\&P} \cdot E[SINR_{i,j\&k=0}^{M\&P}] + Prob_{k=0}^P \cdot E[SINR_{i,k=0}^P] \tag{4.29}$$

4.5 Numerical Results

A mathematical analysis was carried out using the SINR expressions derived in the previous sections. The effect of system parameters on the SINR performance is evaluated for the scenario described in section 4.2.2. Those parameters are:

M_{SH}	soft handover margin
$r_{i,j=0}$	distance from serving Macro eNB to UE
d	distance of Pico eNB from serving Macro eNB
δ	activity factor
mm	Macro eNB pathloss exponent
pmm	Pico eNB pathloss exponent
σ	standard deviation
ε	intra-cell interference coefficient
ISD	inter-site distance between serving eNB and neighbor $j = 1$ -th eNB

The antenna gain and connector loss is 5dBi, however we set the total gain = 0 considering feeder line loss which is 3dB [24]. The parameter $mm = 3.76$ and $pm = 3.67$ are considered in our numerical analysis section, and the parameter $\xi_{i,j} = 8\text{dB}$ and $\xi_{i,k} = 8\text{dB}$ are considered in our numerical analysis.

We analyzed the SINR depending on distance $r_{i,j=0}$ which is the distance between the i -th UE and serving Macro eNB in Fig. 4-6 - 4-12. In order to see the impact on SINR depending on the location of Pico cell, we moved the center of cell from 400 to 200 meter which is closer to the Macro eNB. The parameter d shows the distance

of Pico cell from macro eNB and we put $ISD = 1\text{km}$. We also analyzed the SINR based on fixed distance range from 0 to 500 meter regardless of the location of Pico cell because we want to see the changes of SINR when a UE moved from Macro to Pico (from 0 meter to d), and Pico to Macro (from d to 500meter). And the power of each eNB ($eNB_{j=0}^M, eNB_j^M, eNB_{k=0}^P$) is also changed.

In Fig. 4-6, the SINR depending on distance $r_{i,0}$ is plotted. We considered $d=200$ meter, Power=[46,46,37], $\sigma=8$, and $\varepsilon=0.05$ respectively. The X-axis defines the distance in the range from 0 to 500, where $r_{i,0}=100$ means the cell border between serving eNB and pico eNB. When M_{SH} is varied from 0 to 2dB, and from 2dB to 4dB, the SINR at the cell border is increased by 2dB. Similarly we plotted Fig. 4-7 at 300 meter and Fig. 4-8 at 400 meter where only the location of Pico cell is changed. The plots show that similar SINR gains (about 2dB) at boundary when M_{SH} is varied. The results in Fig. 4-6, Fig. 4-7, and Fig. 4-8 show that the SINR dynamic range is decreased by 3, 4.5 and 6dB respectively when the location of Pico is changed from 400 to 300 and 200 meter. The SINR of a UE is improved due to CoMP gain when the pico cell is placed near Macro. The important target in HO is to increase the lowest SINR values in HO area. The important target in HO is to increase the lowest SINR values in HO area.

In Fig. 4-9 and Fig. 4-10, only the power of Pico cell is changed from 37dBm ($N=1$) to 34dBm ($N=2$), and from 37dBm to 28dBm ($N=4$), the corresponding SINRs at 100 meter are decreased due to the reduced Pico power as expected respectively. And also the SINRs at 500 meter was decreased. One interesting note is that especially for pico to macro case (500 meter)UE requires CoMP gain. And In Fig. 4-11 and

Fig. 4-12, the results show that more CoMP gain is required when the Pico power is reduced. Here SINR $M_{SH}=0$ which means hard handover values can be compared. And in Fig. 4-7, Fig. 4-11, and Fig. 4-12, the SINR range at 200 meter is different. It shows that different M_{SH} should be applied in handover algorithm by different power of pico cell.

In Fig. 4-13, SINR versus M_{SH} for different values of *Power* at 200meter ($d=300$ meter, $\sigma=8$, and $\varepsilon=0.05$) is plotted. It shows the impact of the number of user in Pico cell. In order to achieve the same SINR = 0, the case of Power [46, 46, 34] configuration only needs $M_{SH}=2$ while the case of Power [46, 46, 28] configuration needs $M_{SH}=8$. This shows that a UE requires CoMP gain by 6dB when the number of user in Pico cell increased from N=2 to N=4.

In Fig. 4-14, SINR versus M_{SH} for different values of *Power* at 200 meter ($d=300$ meter, $\sigma=8$, and $\varepsilon=0.05$) is plotted. We show the SINR as the intra-cell interference factor ε is varied. The figure shows that the SINR improves as ε becomes smaller, due to decreased intra-cell interference. The effect of intra-cell interference on SINR is larger for large values of M_{SH} relative to the inter-cell interference, resulting in larger difference in SINR values. Same exercise is performed in Fig. 4-15 in case of Pico to Macro case.

In Fig. 4-16, SINR versus M_{SH} for different values of ρ at 120 meter ($d=300$ meter, $\sigma=8$, and Power=[46,34,34]) is plotted. The figure shows that the SINR improves as ρ becomes smaller, due to decreased inter-cell interference. The ρ is a function of PRB usage in eNB and it requires optimum resource assignment algorithm which is not covered in this dissertation.

The results studied could be applied to system design and deployment, where SINR gain can be achieved by optimizing M_{SH} , depending on propagation condition.

4.6 Conclusion

In this chapter, Heterogeneous network deployment scenarios are being studied and analyzed in the LTE-A. We have derived intra-cell and inter-cell interference models for LTE-A. A mathematical analysis of SINR gain between soft handover and hard handover is carried out based on the Maximal Ratio Combining reception. The results show that propagation, power and the number of in cell significantly influence the choice of M_{SH} and the SINR performance. Therefore this combination of parameters should be considered the choice of M_{SH} in the handover algorithm. The results in this chapter can be used as a guideline in designing and operating the radio network based on LTE-A technology to improve the cell edge user performance. An the analysis of handover gain for different types of heterogeneous network including Home eNBs and Relay Nodes will be the subject of future research.

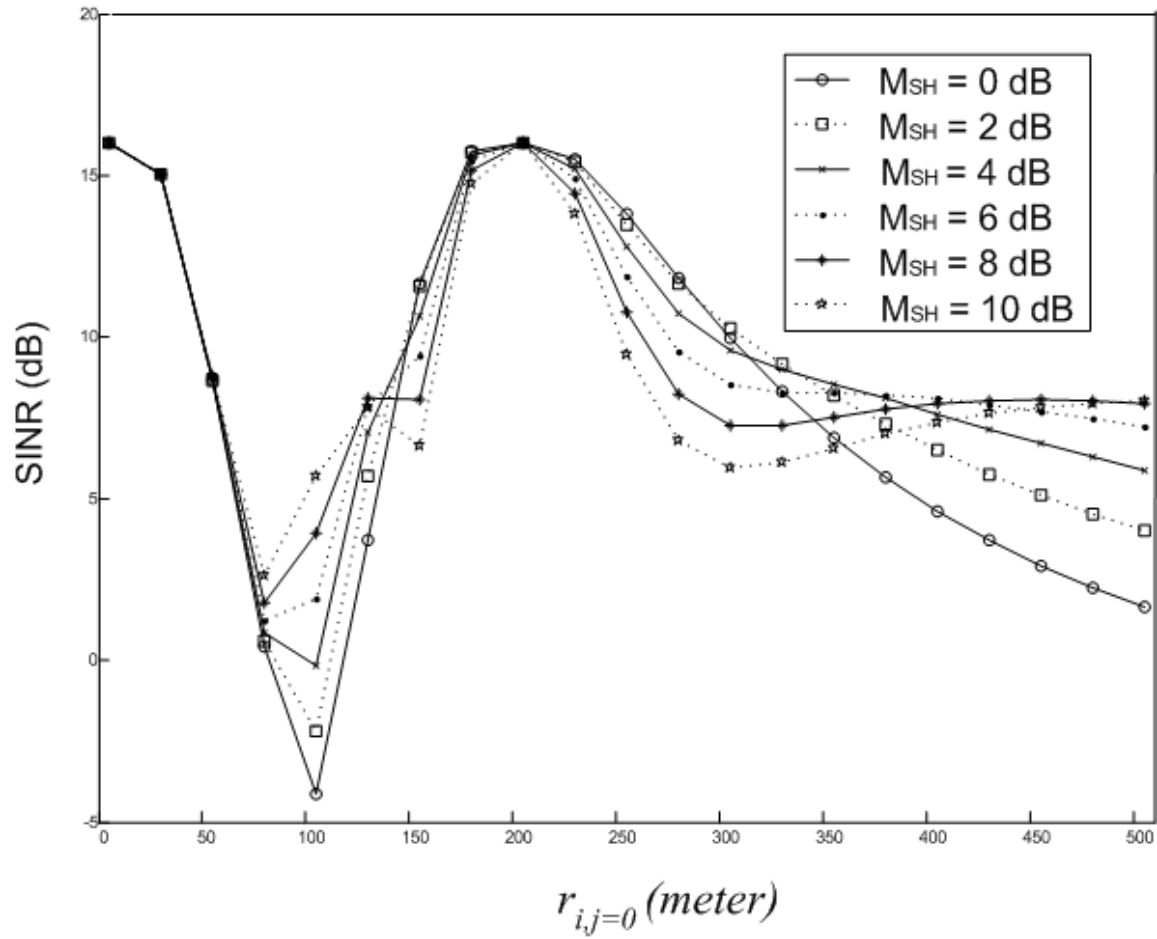


Figure 4-6: SINR depending on distance $r_{i,0}$ ($d=200$ meter, Power=[46,46,37], $\sigma=8$, and $\varepsilon=0.05$)

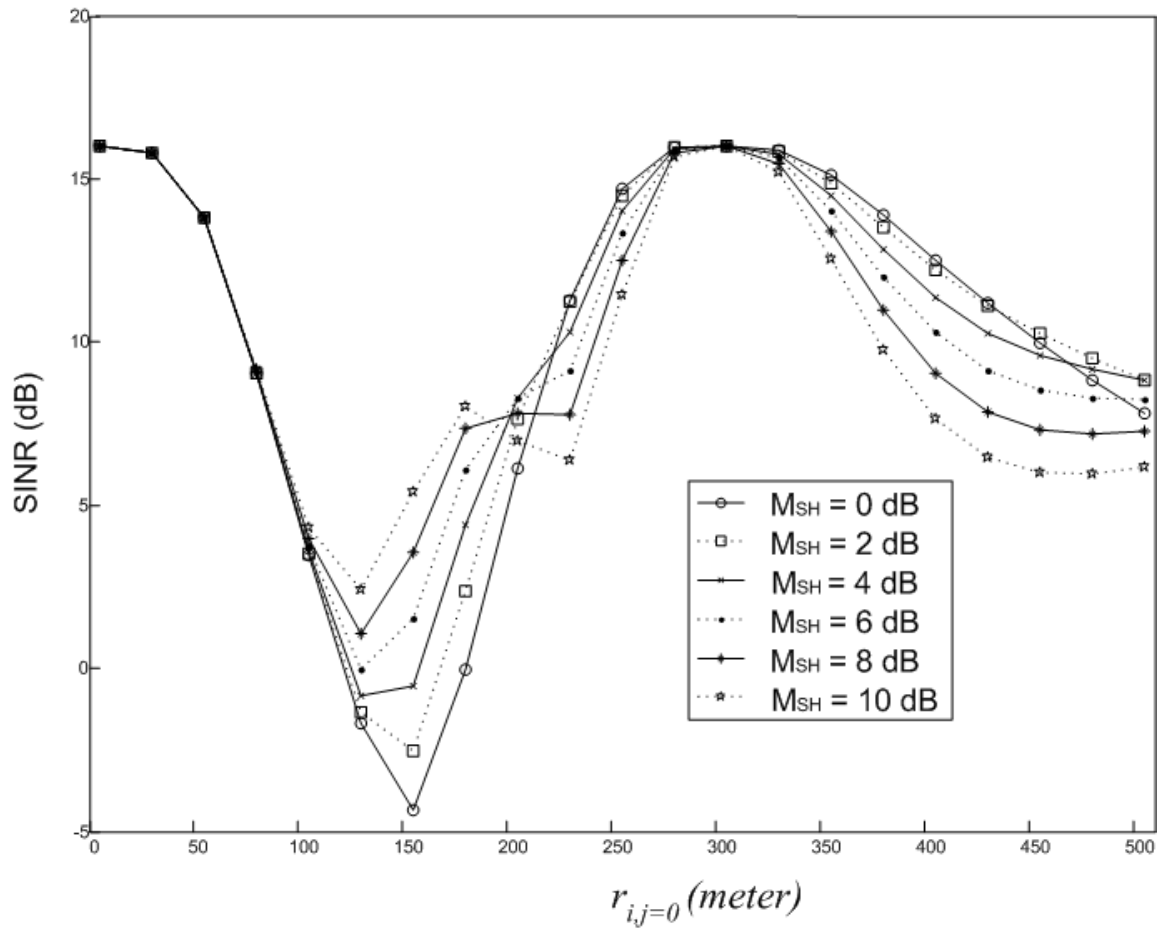


Figure 4-7: SINR depending on distance $r_{i,0}$ ($d=300$ meter, Power=[46,46,37], $\sigma=8$, and $\varepsilon=0.05$)

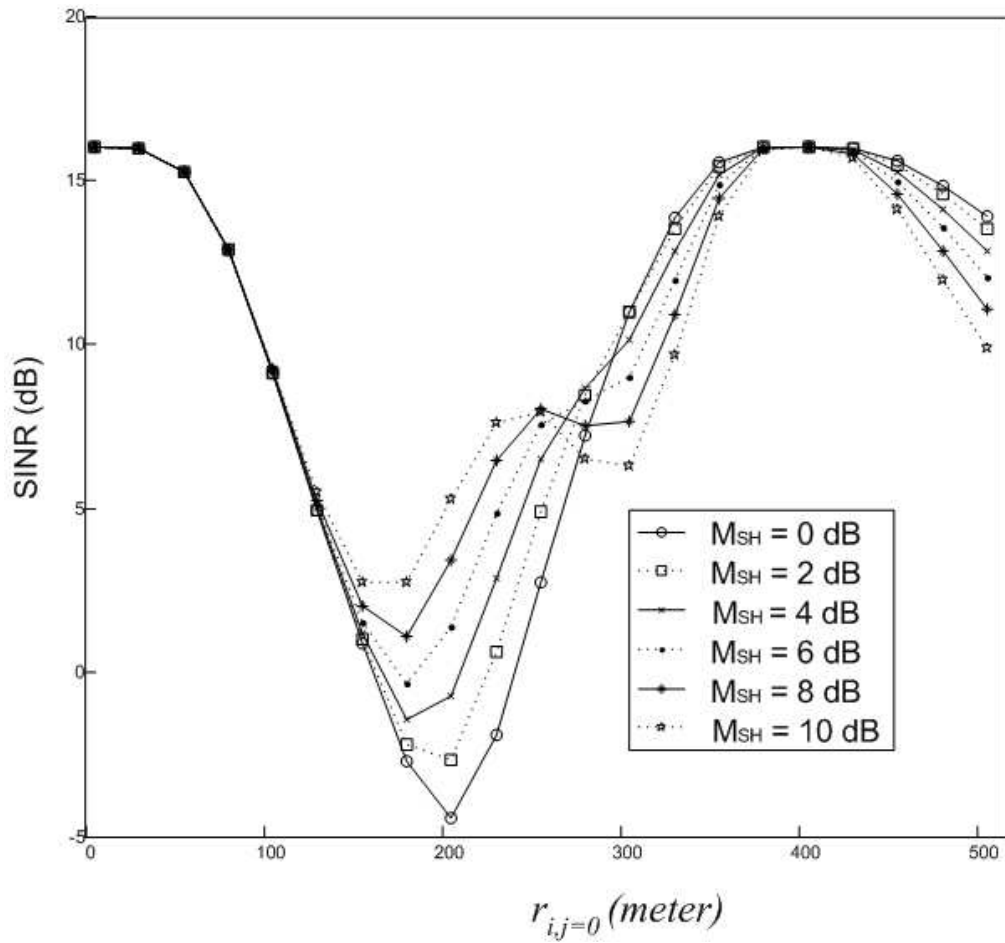


Figure 4-8: SINR depending on distance $r_{i,0}$ ($d=400$ meter, Power=[46,46,37], $\sigma=8$, and $\varepsilon=0.05$)

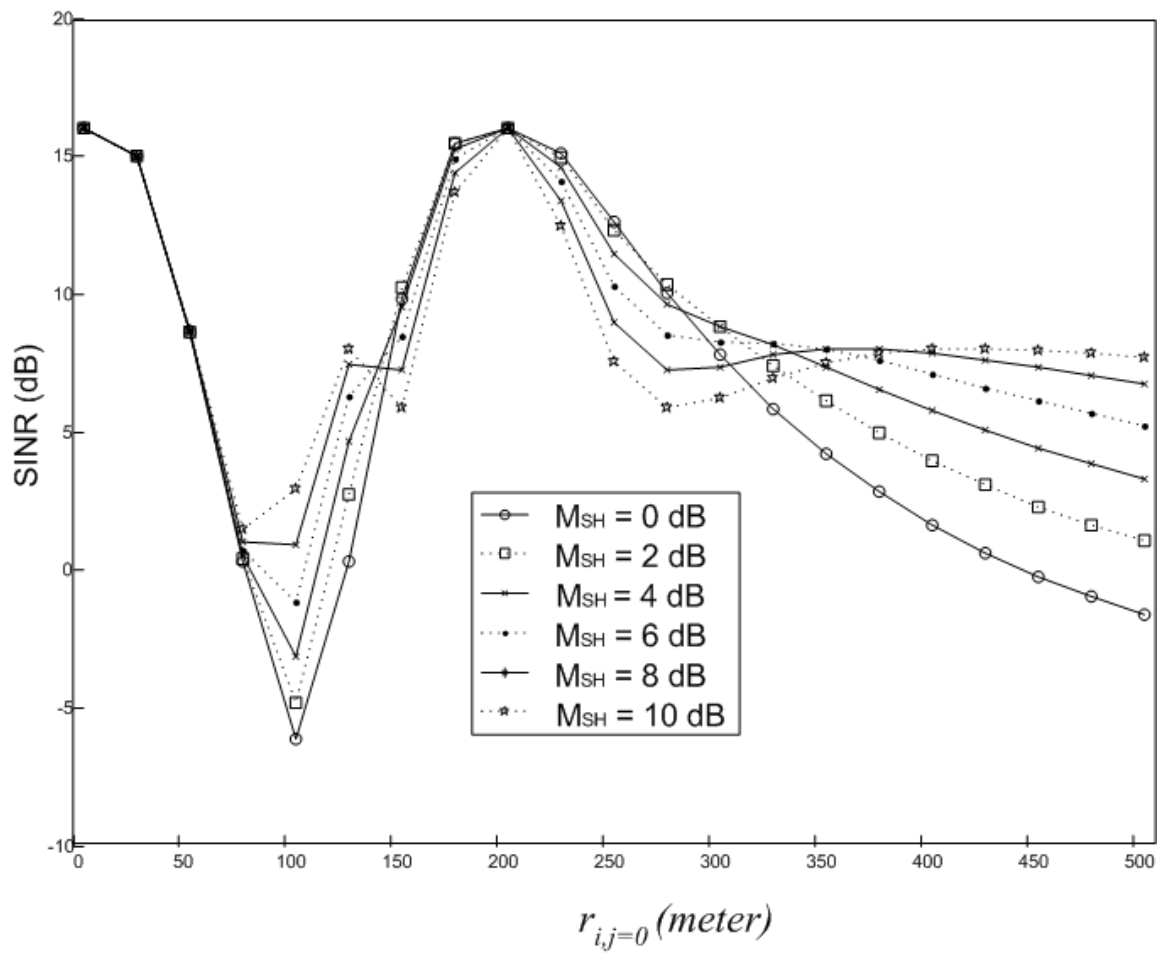


Figure 4-9: SINR depending on distance $r_{i,0}$ ($d=200$ meter, Power=[46,46,34], $\sigma=8$, and $\varepsilon=0.05$)

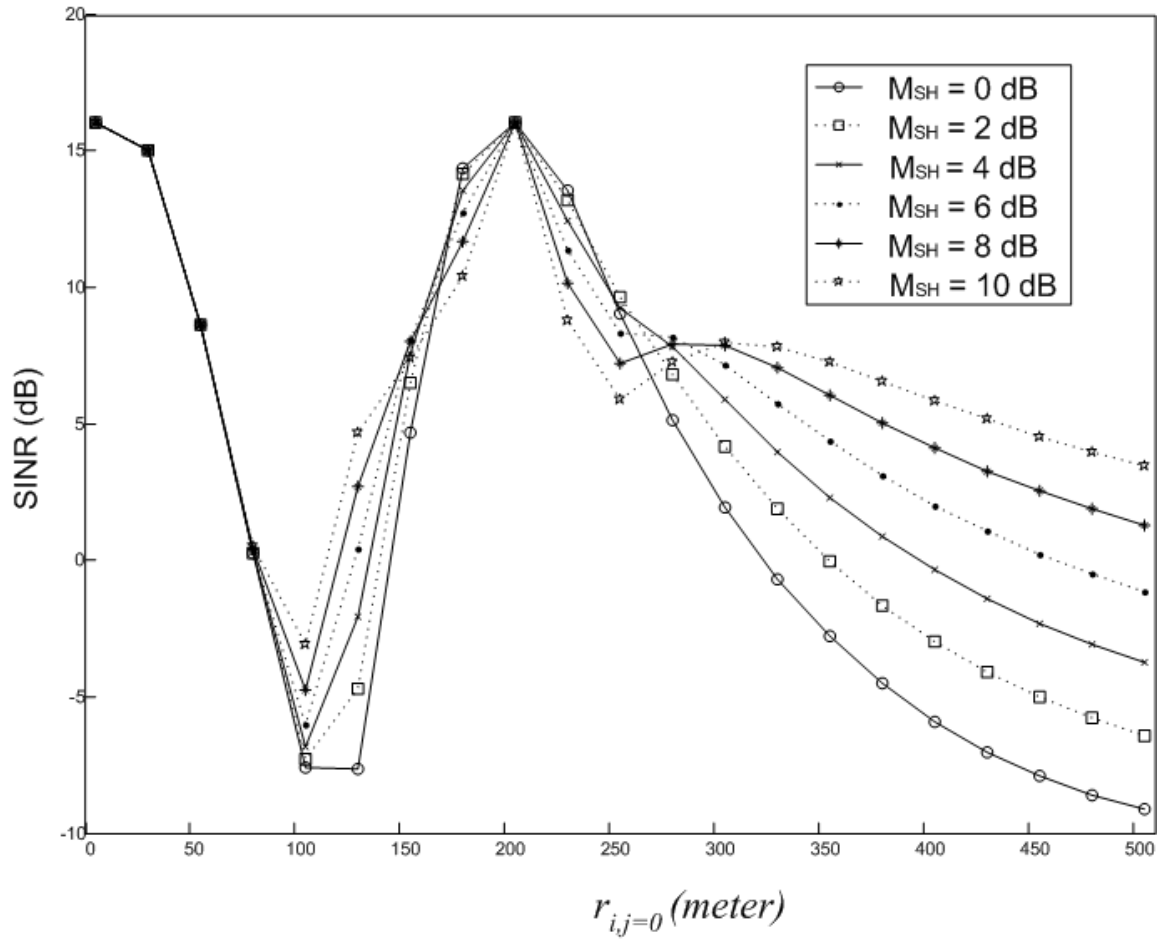


Figure 4-10: SINR depending on distance $r_{i,0}$ ($d=200$ meter, Power=[46,46,25], $\sigma=8$, and $\varepsilon=0.05$)

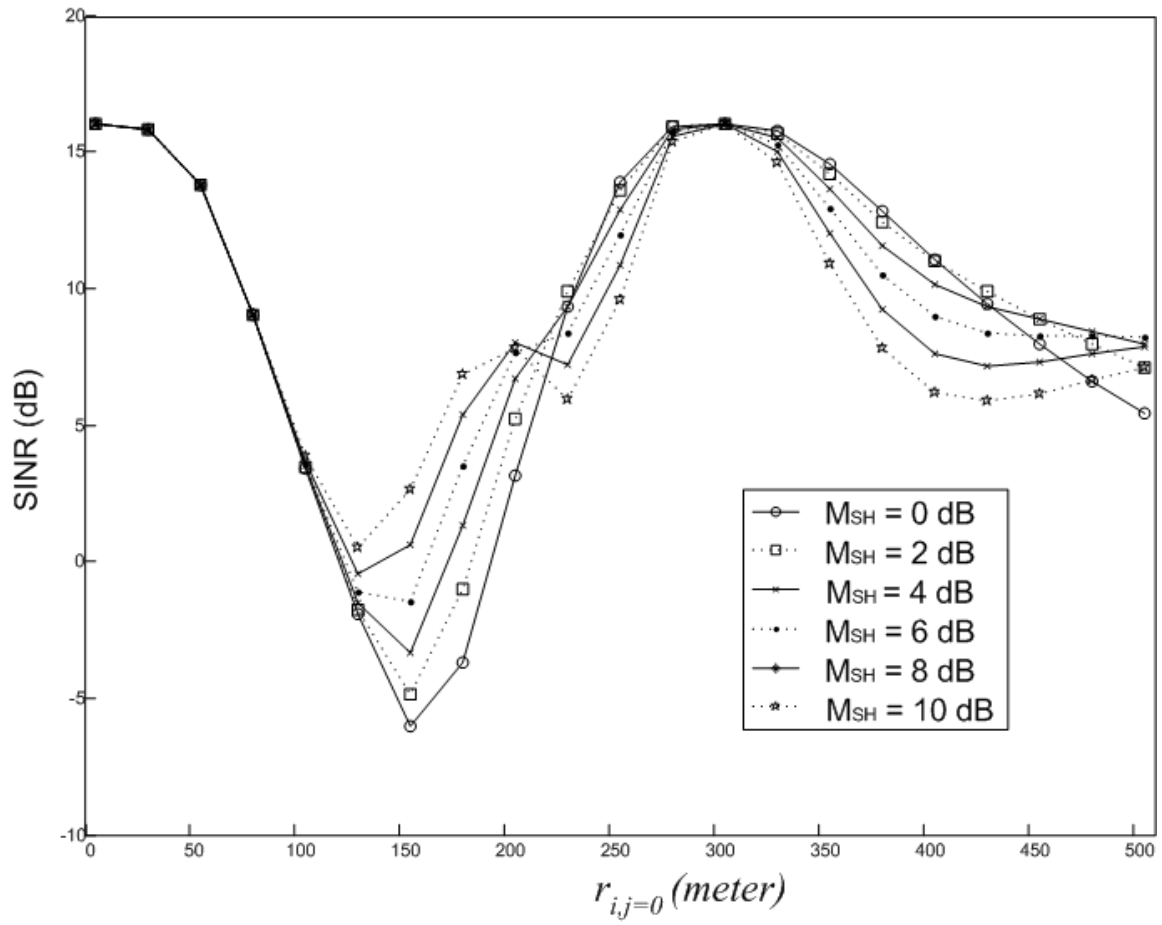


Figure 4-11: SINR depending on distance $r_{i,0}$ ($d=300$ meter, Power=[46,46,34], $\sigma=8$, and $\varepsilon=0.05$)

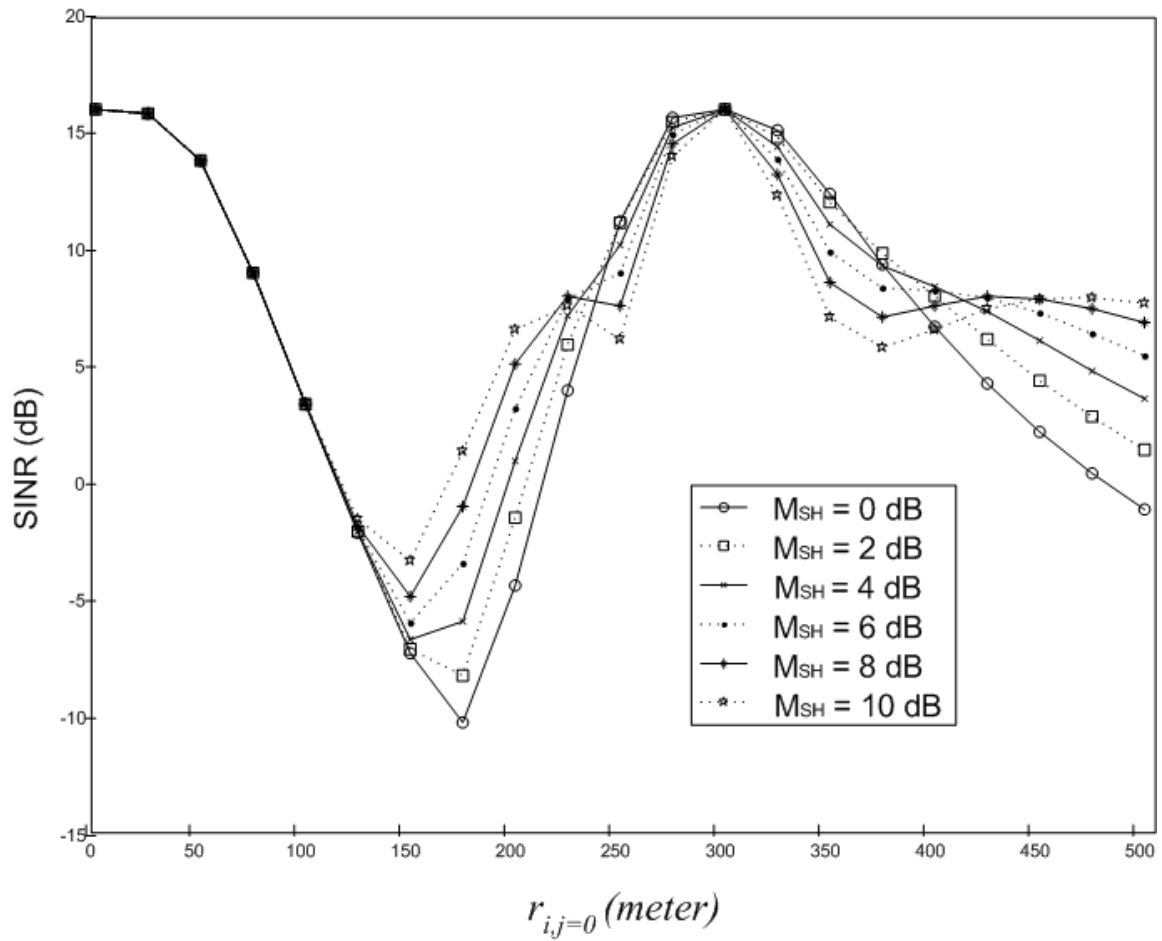


Figure 4-12: SINR depending on distance $r_{i,0}$ ($d=300$ meter, Power=[46,46,28], $\sigma=8$, and $\varepsilon=0.05$)

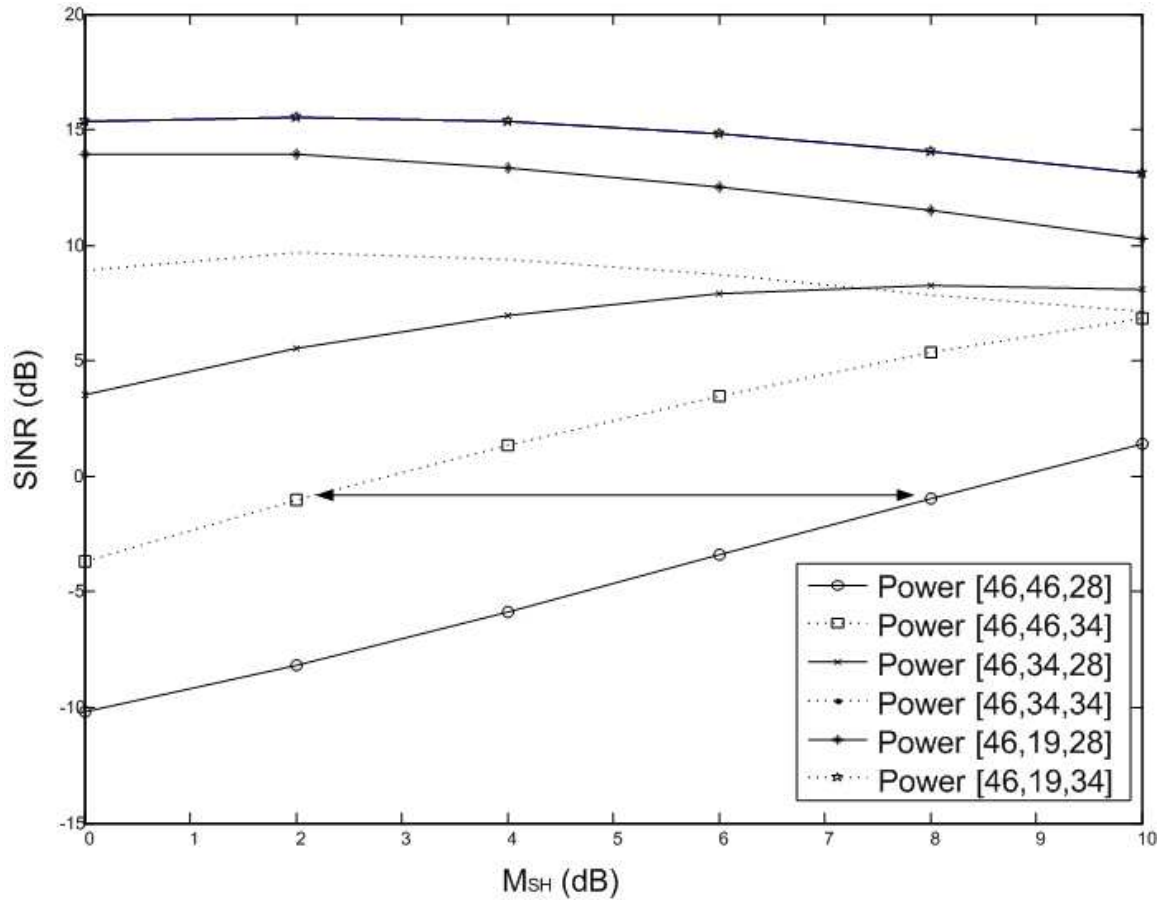


Figure 4-13: SINR versus M_{SH} for different values of $Power$ at 200meter ($d=300$ meter, $\sigma=8$, and $\varepsilon=0.05$)

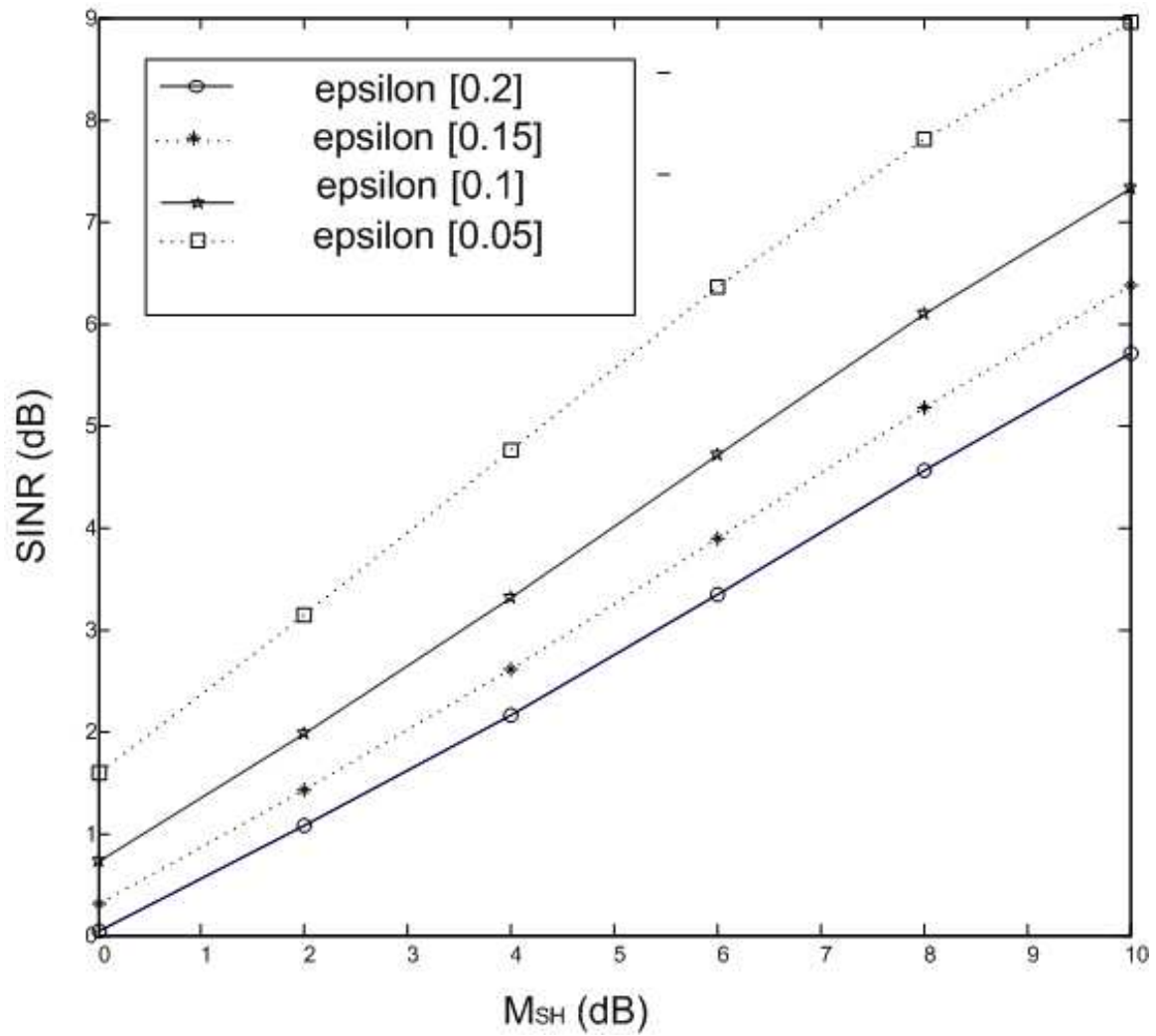


Figure 4-14: SINR versus M_{SH} for different values of ϵ at 120meter ($d=300$ meter, $\sigma=8$, and Power=[46,34,34])

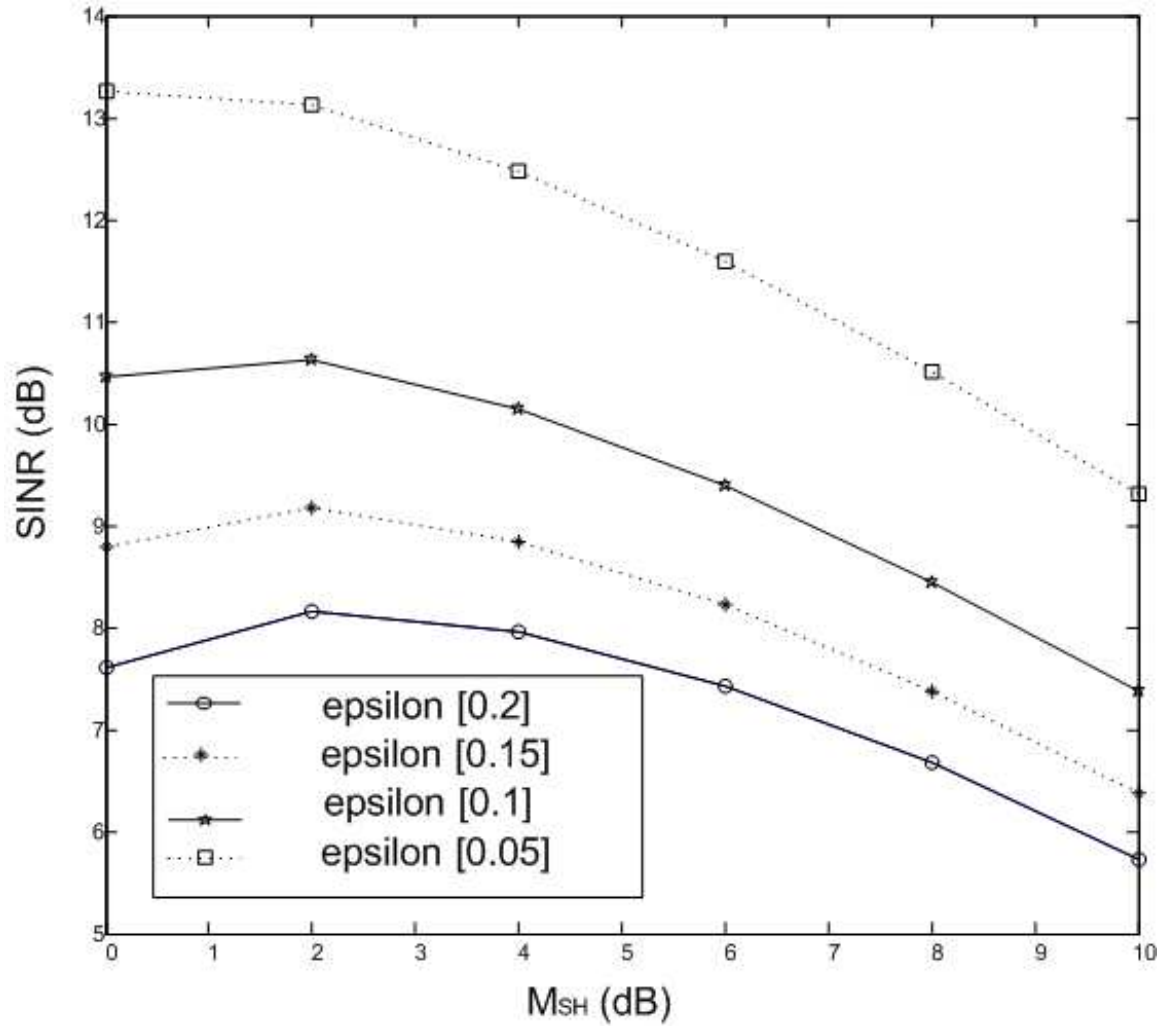


Figure 4-15: SINR versus M_{SH} for different values of ϵ at 500meter ($d=300$ meter, $\sigma=8$, and Power=[46,34,34])

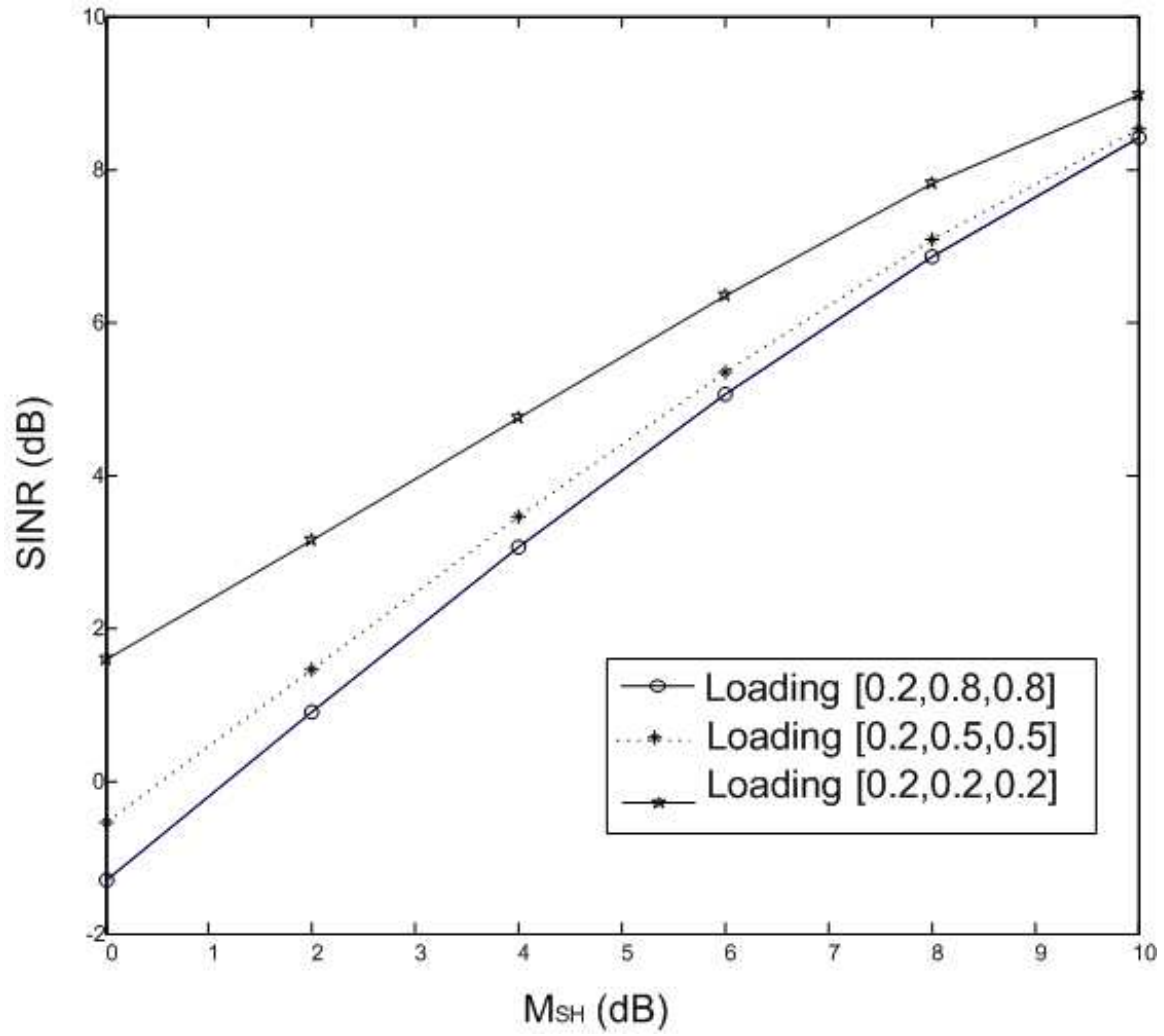


Figure 4-16: SINR versus M_{SH} for different values of ρ at 120meter ($d=300$ meter, $\sigma=8$, and Power=[46,34,34])

Chapter 5

Conclusion and Future Research

5.1 Conclusion

In this dissertation, we have analyzed the macro-diversity gain of that can be achieved in the LTE-A system. Homogeneous network deployment scenarios are being studied. We have derived intra-cell and inter-cell interference models for LTE. A mathematical analysis of SINR gain between soft handover and hard handover is carried out based on the Maximal Ratio Combining reception. The results show that propagation parameters significantly influence the choice of M_{SH} and the SINR performance.

Heterogeneous network deployment scenarios are also being studied in the LTE-A. One of objectives is to provide seamless mobility in the mixed case of macro and pico eNBs in co-channel deployment scenario where the RF coverage areas may be overlapped. Support of heterogeneous network will require the modification of radio link connection approach due to coverage imbalance between DL and UL by the different transmit powers of macro and pico eNBs. In a conventional network

including LTE Release 8, the UE is typically connected to the cell that provides the strongest DL signal power. However, the UE suffers from strong interference due to UL/DL link imbalance in a heterogeneous network. We investigate possible solutions to address this issue based on analytical framework and characterized RF parameters based on collaborative transmission.

The results in this chapter can be used as a guideline in designing and operating the radio network based on LTE-A technology to improve the cell edge user performance.

5.2 Future research

Our analysis for homogeneous and heterogeneous network scenarios in LTE-A system is based on a simple linear topology with two eNBs and it is performed in the CoMP set. We will extend this scenarios to multiple cell deployment including heterogeneous network. And the algorithm will be further enhanced by self-optimization framework. The simulation tool will be developed to compare and demonstrate the handover performance with KPIs including call statistics.

And the analysis of handover gain for different types of heterogeneous network including Home eNBs and Relay Nodes will be the subject of future research.

Bibliography

- [1] 3GPP E-UTRAN Self-configuring and self-optimizing network use cases and solutions. TR 36.902, 2008
- [2] SOCRATES, Self-optimisation and self-configuration in wireless networks, European Research Project, <http://www.fp7-socrates.eu.org>.
- [3] 3GPP, Self-configuring and self-optimizing network use cases and solutions, Technical Report TR 36.902
- [4] K. M. Rege, S. Nanda, C. F. Weaver, and W.-C. Peng, Analysis of fade margins for soft and hard handoffs, in Proceedings of the 6th IEEE International Symposium on Personal, Indoor and Mobile Radio Communications (PIMRC 95), vol. 2, pp. 829-835, Toronto, Canada, September 1995.
- [5] Z. Liu, Y. Wang, D. Yang, "Effect of Soft Handoff Parameters and Traffic Loads on Soft Handoff Ratio in CDMA System, Analysis of fade margins for soft and hard handoffs, in Proceedings of ICCT2003.
- [6] RP-090536 "New SI proposal: LTE heterogeneous network deployments" Qualcomm. Nokia, NSN.
- [7] 3GPP, <http://www.3gpp.org/>
- [8] 3GPP TR 36.814 V1.1.1, "Further Advancements for E-UTRA-Physical Layer Aspects," June 2009
- [9] A. J. Viterbi, Audrey M. Viterbi, Klein S. Gihousen, and Ephraim Zehavi, Soft handoff extends CDMA cell coverage and increase reverse link capacity, IEEE Journal On Selected Areas In Commun., vol. 12, no. 8, pp. 1281-1288, October 1994. A. J. Viterbi, Audrey
- [10] M. Viterbi, and Ephraim Zehavi, Other-Cell Interference in Cellular Power-Controlled CDMA, IEEE Trans. on Communication, vol. 42, no. 2314, pp. 1501-1504. Feb. 1994.
- [11] D. Wong and T. J. Lim, Soft handoffs in CDMA mobile systems, IEEE Personal Commun., vol. 4, no. 6, pp. 6-17, Dec. 1997.

- [12] Jung Ah C. Lee, Coordinated Multi-Point transmission in 3GPP LTE-Advanced,” in Proc. The 24th international conference on circuits/systems, computers and communications, Jeju, Korea, 2009.
- [13] HK Lee, HS Son and Sanghoon Lee, Semisoft Handover Gain Analysis Over OFDM-Based Broadband Systems, IEEE Trans. on Vehicular, 2009,vol. 58, pp. 1443-1453.
- [14] C.Mihailescu, X. Lagrange, and P. Godlewski, Soft handover analysis in downlink UMTS WCDMA system, in Proc. IEEE MoMuC, San Diego, CA, 1999, pp. 279285.
- [15] Pedersen, K.I.; Kolding, T.E.; Frederiksen, F.; Kovacs, I.Z.; Laselva, D.; Mogensen, P.E, An Overview of Downlink Radio Resource Management for UTRAN Long-Term Evolution” IEEE Comm. Magazine, 2009, vol. 47, pp. 86-93.
- [16] D. Aziz, R. Single, Improvement of LTE Handover Performance through Interference Coordination, Vehicular Technology Conference, 2009. VTC Spring IEEE 69th 26-29, pp. 1-5, April 2009.
- [17] R1-091687, ”Discussion on the relation between CoMP cooperating set and CoMP reporting set”, NEC, 3GPP TSG-RAN WG1 57, San Francisco, USA, 4th - 8th May, 2009.
- [18] R1-091688, ”Potential gain of DL CoMP with Joint transmission”, NEC, 3GPP TSG-RAN WG1 57, San Francisco, USA, 4th - 8th May, 2009.
- [19] 3GPP TR 36.814, ”Further enhancements for E-UTRA-Physical Layer Aspects”, 2009.
- [20] RP-090536 ”New SI proposal: LTE heterogeneous network deployments” Qualcomm. Nokia, NSN.
- [21] R1-093787 ”Scenarios for Heterogeneous Network for LTE-A”, Alcatel-Lucent, Alcatel-Lucent Shanghai Bell.
- [22] D. Ghosh, C. Lott, Uplink-Downlink Imbalance in Wireless Cellular Network, IEEE International Communications Conference, pp. 4275-4280, June 2007.
- [23] Morimoto, A., Tanno, M., Kishiyama, Y., Higuchi, K., and Sawahashi, M., Investigation on Optimum Radio Link Connection Using Remote Radio Equipment in Heterogeneous Network for LTE-Advanced, Vehicular Technology Conference, 2009. VTC Spring 2009. IEEE 69th
- [24] 3GPP TR 36.814, ”Further enhancements for E-UTRA-Physical Layer Aspects”, V9.0.0 2010.